



HAL
open science

Tajik Basin and Southwestern Tian Shan, Northwestern India-Asia Collision Zone: 1. Structure, Kinematics, and Salt Tectonics in the Tajik Fold-and-Thrust Belt of the Western Foreland of the Pamir

Łukasz Gałala, Lothar Ratschbacher, Jean-Claude Ringenbach,
Sofia-Katarina Kufner, Bernd Schurr, Ralf Dedow, Sanaa Abdulhameed,
Edouard Le Garzic, Mustafo Gadoev, Ilhomjon Oimahmadov

► To cite this version:

Łukasz Gałala, Lothar Ratschbacher, Jean-Claude Ringenbach, Sofia-Katarina Kufner, Bernd Schurr, et al.. Tajik Basin and Southwestern Tian Shan, Northwestern India-Asia Collision Zone: 1. Structure, Kinematics, and Salt Tectonics in the Tajik Fold-and-Thrust Belt of the Western Foreland of the Pamir. *Tectonics*, 2020, 10.1029/2019TC005871 . insu-02873593

HAL Id: insu-02873593

<https://insu.hal.science/insu-02873593>

Submitted on 18 Jun 2020

HAL is a multi-disciplinary open access archive for the deposit and dissemination of scientific research documents, whether they are published or not. The documents may come from teaching and research institutions in France or abroad, or from public or private research centers.

L'archive ouverte pluridisciplinaire **HAL**, est destinée au dépôt et à la diffusion de documents scientifiques de niveau recherche, publiés ou non, émanant des établissements d'enseignement et de recherche français ou étrangers, des laboratoires publics ou privés.

Tectonics

RESEARCH ARTICLE

10.1029/2019TC005871

This article is a companion to Dedow et al. (2020) <https://doi.org/10.1029/2019TC005874>, Abdulhameed et al. (2020) <https://doi.org/10.1029/2019TC005873>.

Key Points:

- Surface, seismic, and borehole data show ≥ 150 -km, thin-skinned Tajik-basin shortening at $\sim 90^\circ$ to the India-Asia convergence direction
- Structural geometries vary due to the buttressing by the surrounding thick-skinned belts and variable Jurassic salt thickness and facies
- Structures include flat-ramp thrust sheets, piggy-back and break-back thrusts, faulted detachment folds, salt sheets, and squeezed diapirs

Supporting Information:

- Supporting Information S1
- Figure S1
- Figure S2
- Figure S3
- Figure S4
- Figure S5
- Figure S6
- Figure S7
- Figure S8

Correspondence to:

L. Ratschbacher,
lothar@geo.tu-freiberg.de;
lukasz.gagala@hotmail.com

Citation:

Gagała, L., Ratschbacher, L., Ringenbach, J.-C., Kufner, S.-K., Schurr, B., Dedow, R., et al. (2020). Tajik basin and southwestern Tian Shan, northwestern India-Asia collision zone: 1. Structure, kinematics, and salt tectonics in the Tajik fold-and-thrust belt of the western foreland of the Pamir. *Tectonics*, 39, e2019TC005871. <https://doi.org/10.1029/2019TC005871>









Received 3 SEP 2019

Accepted 12 FEB 2020

Accepted article online 18 MAR 2020

©2020. American Geophysical Union.
All Rights Reserved.

Tajik Basin and Southwestern Tian Shan, Northwestern India-Asia Collision Zone: 1. Structure, Kinematics, and Salt Tectonics in the Tajik Fold-and-Thrust Belt of the Western Foreland of the Pamir

Łukasz Gagała^{1,2} , Lothar Ratschbacher¹ , Jean-Claude Ringenbach³, Sofia-Katarina Kufner⁴ , Bernd Schurr⁴ , Ralf Dedow¹ , Sanaa Abdulhameed¹ , Edouard Le Garzic³ , Mustafó Gadoev⁵ , and Ilhomjon Oimahmadov⁵

¹Geologie, Technische Universität Bergakademie Freiberg, Freiberg, Germany, ²Now at Hellenic Petroleum, Marousi, Greece, ³E2S-UPPA, CNRS, University of Pau and Pays de l'Adour, Pau, France, ⁴German Research Center for Geosciences, Potsdam, Germany, ⁵Institute of Geology, Earthquake Engineering and Seismology, Tajik Academy of Sciences, Dushanbe, Tajikistan

Abstract Surface, seismic, and borehole data characterize the Neogene-Recent Tajik fold-and-thrust belt of the Tajik basin. The basin experienced little sub-detachment basement deformation, acting as a rigid foreland plate during the Pamir orogeny. The Tajik fold-and-thrust belt contains variable thin-skinned structural styles, changing along and across strike as a function of the thickness and facies of Upper Jurassic evaporites, which constitute the basal detachment, and the influence of the surrounding thick-skinned belts. The southern Tajik fold-and-thrust belt shows regularly spaced, salt-cored, thrust detachment anticlines that transition northward into imbricated thrust sheets grouped in oppositely verging stacks facing each other across a common footwall syncline. The width of the fold-and-thrust belt decreases northeastward accommodated by the Ilyak fault, a lateral ramp developed over a seismically active dextral basement fault. The southeastern Tajik fold-and-thrust belt contains massive subaerial salt sheets, formed by squeezing of preexisting salt diapirs. The salt-tectonic domain originates from a local depocenter within the Late Jurassic Amu Darya-Tajik evaporitic basin. Serial cross sections, integrating the structural geometries, yielded minimum thin-skinned shortening oriented at $\sim 90^\circ$ to the India-Asia convergence direction, increasing from ~ 93 km in the south to ~ 148 km in the center, and dropping to ~ 22 km in the northeast; total shortening—including the foreland buttress—is ≥ 170 km. Most of the shortening in the central-southern Tajik fold-and-thrust belt occurred by hinterland-vergent, high-displacement back thrusts. The Pamir played a dominant role in the transfer of shortening to the sedimentary infill of the Tajik basin with the Tian Shan acting as a semi-passive buttress.

1. Introduction

The Tajik basin is the eastern extension of the greater Amu Darya basin, situated in a retrowedge position with respect to the India-Asia collision zone (Figure 1a). It evolved from a Triassic-Eocene epicontinental sag basin into an Oligocene-Recent foreland basin of the Pamir and Tian Shan (e.g., Brookfield & Hashmat, 2001; Carrapa et al., 2015; Chapman et al., 2019; Dedow et al., 2020; Klocke et al., 2017; Nikolaev, 2002). At present, the Tajik basin links to the Amu Darya basin through a narrow corridor between the southwestern termination of the Tian Shan and the Afghan platform (Figure 1b). Detached along Upper Jurassic evaporites, its strata form the Tajik fold-and-thrust belt (FTB) locked between the Pamir and the western Tian Shan; the latter is referred to as the Uzbek and Tajik Gissar (Figure 1b; e.g., Bekker, 1996; Burtman & Molnar, 1993; Bourgeois et al., 1997; Thomas, Chauvin, et al., 1994; Thomas, Gapais, et al., 1994).

The Tajik FTB involves ~ 5 - to 10-km-thick, Upper Jurassic-Recent strata (Figure 1b; e.g., Bekker, 1996; Burtman & Molnar, 1993; Bourgeois et al., 1997; Chapman et al., 2017). The Pamir constitutes its hinterland backstop, the Tajik Gissar and Afghan platform the northern and southern lateral buttresses, respectively, and the Uzbek Gissar the frontal buttress. GPS velocity vectors (Figure 1c; e.g., Ischuk et al., 2013; Perry et al., 2019; Zubovich et al., 2010) and crustal seismicity (Figure 1b; Kufner et al., 2018; Schurr

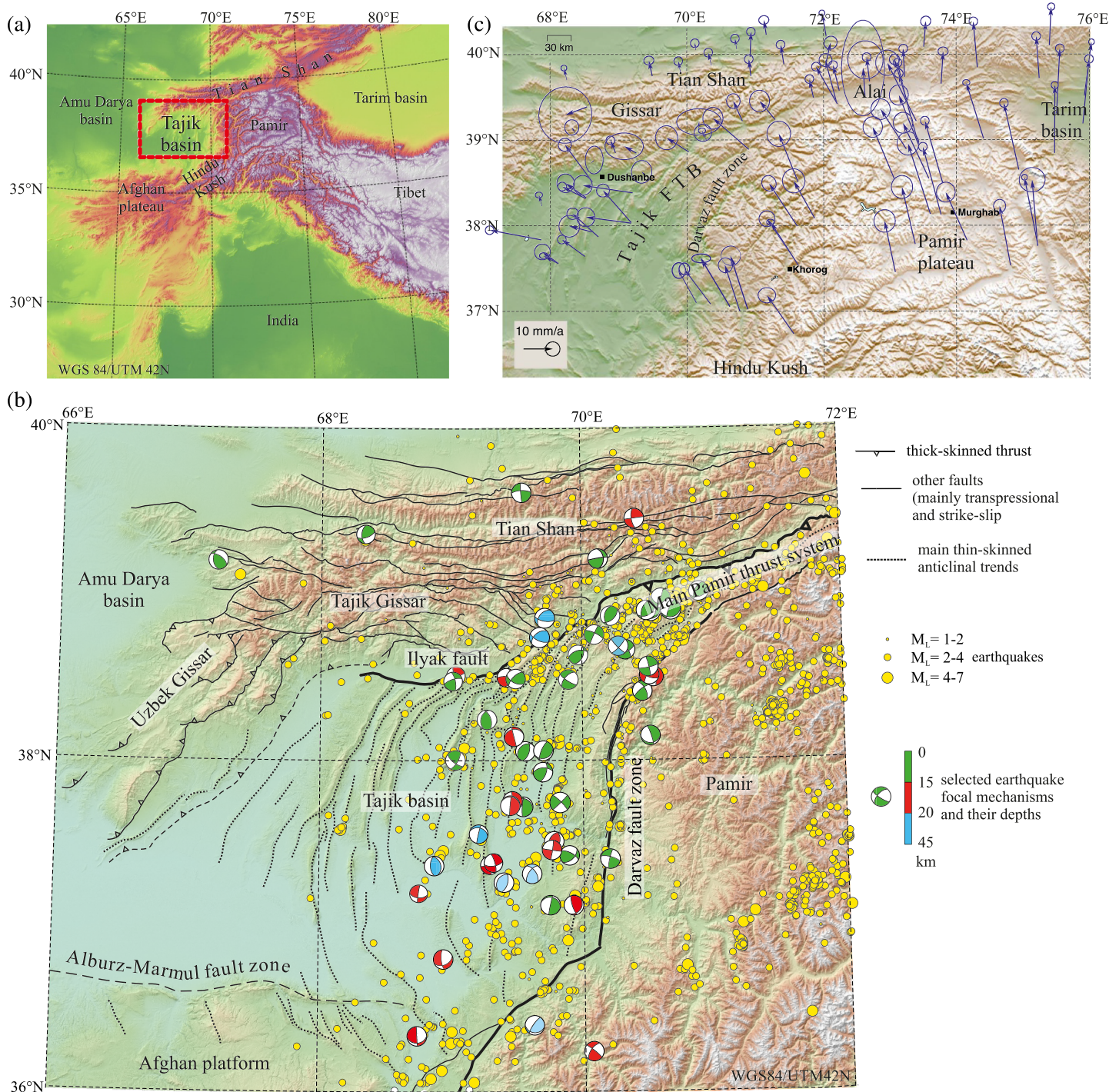


Figure 1. (a) Location of the Tajik basin at the northwestern tip of the India-Asia collision zone. (b) Crustal seismicity and selected earthquake focal mechanism (Kufner et al., 2018, for the full data set), plotted on top of a new map of the Cenozoic structures of the Tajik basin and its surrounding mountain belts. Structures interpreted from the 1:200,000 geologic maps (GRI, 1961–1984), Vlasov et al. (1991), Doebrich and Wahl (2006), and our new subsurface data. Trace of the Darvaz fault is an approximation of a more complex fault zone with several overlapping and anastomosing segments. (c) GPS velocity vectors (Ischuk et al., 2013; Perry et al., 2019; Zubovich et al., 2010).

et al., 2014) indicate that the Pamir moves north relative to stable Asia with little internal deformation in its eastern part. The western Pamir shows higher seismic deformation, expressed by strike-slip and normal faults, indicating ~E-W extension together with ~N-S shortening. Seismicity is concentrated along the

Main Pamir thrust system, where the Pamir's northern margin thrusts over the Alai valley—remnant of a Mesozoic-Paleogene Amu Darya-Tajik-Tarim basin system (Figures 1a and 1b; e.g., Sippl et al., 2014). The GPS vectors turn from ~NNW in the eastern Pamir to ~WNW in the Tajik basin (Figure 1c). Schurr et al. (2014) and Kufner et al. (2018) interpreted this deformation field as a combination of bulk northward displacement and westward collapse of the Pamir-plateau crust; the westward advance is accommodated by ~E-W shortening in the Tajik basin (Figure 2a). The seismicity along the northern and eastern rims of the Tajik basin shows transpressive dextral strike-slip kinematics along the Ilyak fault and sinistral strike-slip kinematics along the Darvaz fault zone, respectively (Figure 1b). In the south, deformation occurs beneath the Afghan platform, where hypocenters reach ~40-km depth. Seismicity in the interior of the Tajik basin clusters in its eastern part, proximal to the Pamir. There, it shows a mixture of strike-slip and thrust kinematics (Figure 1b; Kufner et al., 2018).

Although the structure of the Tajik basin has been the focus of several studies (Bekker, 1996; Bourgeois et al., 1997; Burtman, 2000; Burtman & Molnar, 1993; Chapman et al., 2017; Hamburger et al., 1992; Leith & Alvarez, 1985; Pavlis et al., 1997; Thomas, Chauvin, et al., 1994; Thomas et al., 1996; Thomas, Gapais, et al., 1994), the lack of published subsurface data resulted in diverse structural models. Concepts span from entirely thin-skinned (Bekker, 1996; Burtman, 2000) to hybrid thin- and thick-skinned with various degrees of cover-basement coupling (Bourgeois et al., 1997; Chapman et al., 2017; Thomas et al., 1996; Thomas, Gapais, et al., 1994). These models imply different amounts of ~E-W shortening, mostly as a function of the involvement and depth of the sub-*evaporite* basement. The end-member estimates vary from ~65–70 km (Chapman et al., 2017) to ~240 km (Bourgeois et al., 1997), providing conflicting constraints on the amount of the westward advance of the Pamir salient at the cost of the Tajik-basin crust. This wealth of scenarios reflects the uncertainty on the subsurface geometry of the Tajik basin.

Herein, we present new surface and subsurface constraints on the structure of the Tajik FTB, including a rich borehole database and regional 2-D seismic profiles. These define the basement depth and geometry, structural styles, and their variations throughout the Tajik FTB. A series of regional cross sections integrates the available data, depicts structural geometries, and quantifies the ~ENE-WSW shortening. Incorporation of regional seismicity data (Kufner et al., 2018) further constrains deep geometries and modern kinematics. Thus, our aim is to provide a well-constrained and detailed description of the Tajik FTB. With a map-view restoration of the external edge of the Pamir orocline and a crustal-scale cross section, we illustrate the constraints imposed by the Tajik FTB foreland shortening on the geometry of the Tajik-basin lithosphere beneath the Pamir. Complementary, part 2 of this paper series (Abdulhameed et al., 2020) reports the timing of Tajik FTB formation using thermochronology; part 3 (Dedow et al., 2020) outlines the pre- to syn-orogenic Tajik-basin evolution at its eastern margin.

2. Stratigraphy and Structural Framework of the Tajik Basin and the Southwestern Tian Shan

The Tajik basin hosts a bipartite sedimentary succession (Figure 3). The ?Triassic-Eocene part represents an epicontinental basin (e.g., Burtman, 2000; Nikolaev, 2002). This series consists of mixed, clastic-carbonate lithologies with an important evaporite level—the Late Jurassic Gaurdak Formation (short Fm)—that forms the principal detachment of the Tajik FTB. The massive limestone horizon of the Bukhara Fm occurs near the top, forming a basin-wide correlation horizon and seismic marker. The thickness of the Cretaceous-Eocene post-salt section exposed throughout the Tajik basin is >2.5 km. The depositional thickness of the Gaurdak Fm detachment horizon is not constrained, but seismic data support a >1-km maximum thickness. Pre-salt Triassic-Oxfordian series are exposed in the Gissar where they attain ≤ 1 km. The Oligocene-Recent foreland-basin series consists of continental, syn-orogenic clastic rocks dominated by conglomerates (e.g., Bosov, 1972; Chapman et al., 2019; Dedow et al., 2020; Klocke et al., 2017; Schwab et al., 1980; Sherba, 1990); the thickness of the syn-orogenic strata varies across the basin from ~5 to 7.5 km.

In most cases, the seismic images can be interpreted in terms of stratigraphy (Figure 3). The Oligocene-Recent clastic rocks are either seismically transparent or appear as high-frequency seismic facies. The Lower Cretaceous-Eocene strata are represented by a ~1-s TWT thick package of high-amplitude reflectors, traceable in all lines. The Upper Jurassic evaporites show low-amplitude characteristics when in an

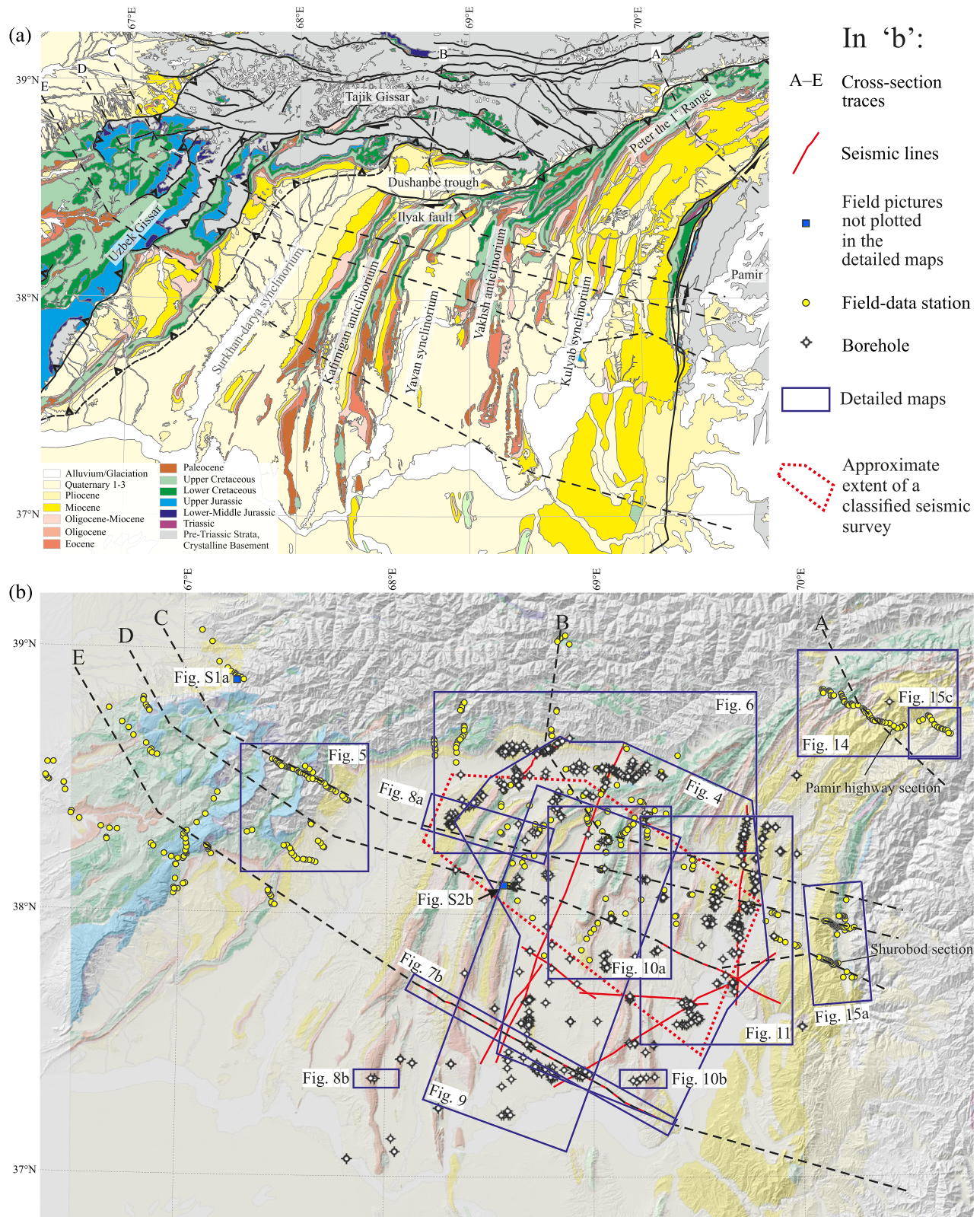


Figure 2. (a) Geologic map of the Tajik basin and surrounding mountain ranges; map sources, see Figure 1. Selected major faults show thick-skinned (basement-involved) structures rimming the thin-skinned Tajik fold-and-thrust belt. The easternmost thrust of the Uzbek Gissar is speculative (see text). Dashed lines A to E represent traces of the regional cross sections of Figure 16. Coordinate system is that of the 1:200,000 maps: SK-42 also known as the Krasovsky 1940 ellipsoid. (b) Base map with key data sets and locations of figures. Coordinate system: WGS84/UTM34N.

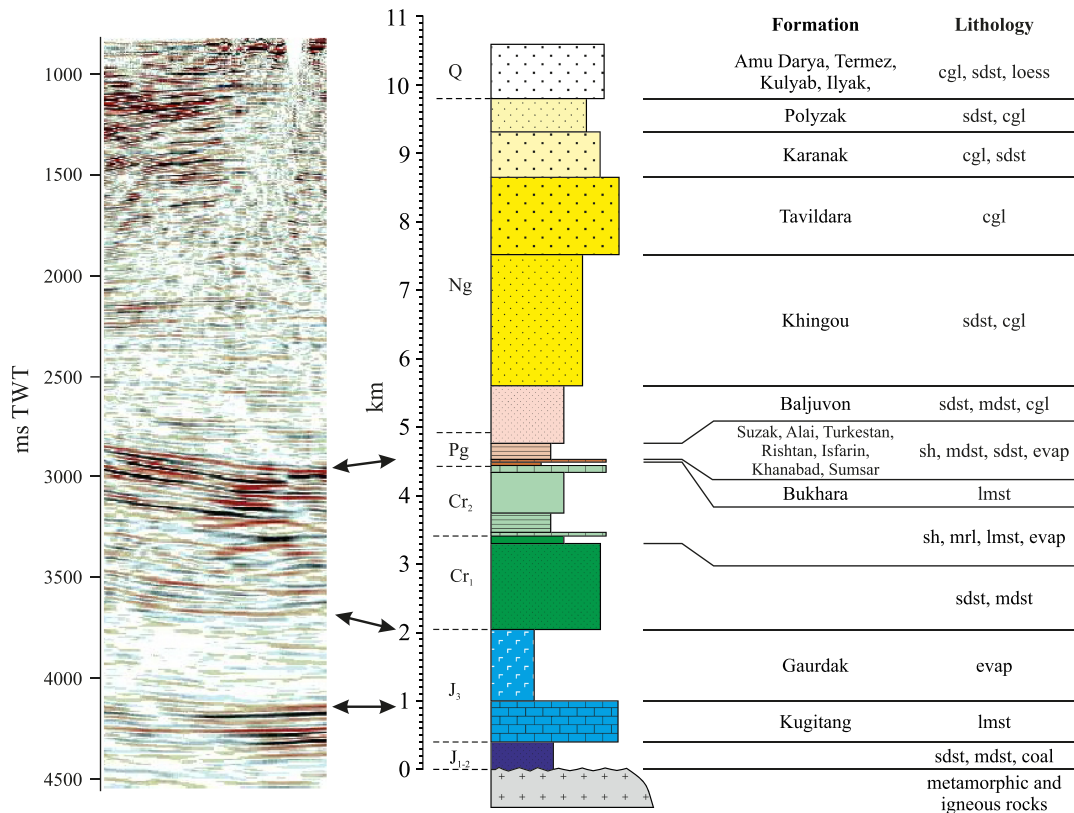


Figure 3. Generalized stratigraphy and seismic facies in the Tajik basin. Formation names are from the Soviet literature (see Dedow et al., 2020, for an overview). Thicknesses are close to reported maximum values. Abbreviations: cgl = conglomerate; sdst = sandstone; mdst = mudstone; sh = shale; mrl = marl; lmst = limestone; evap = evaporite.

original stratigraphic position and are transparent when allochthonous. The base of the evaporite series is seismically imaged only exceptionally, usually as a single, high-amplitude reflector.

The first-order internal structure of the Tajik FTB is known from geologic mapping and structural studies (e.g., Bekker, 1996; Bourgeois et al., 1997; Burtman, 2000; GRI, 1961–1984 [supporting information S1]; Hamburger et al., 1992; Leith & Alvarez, 1985; Nikolaev, 2002; Thomas, Chauvin, et al., 1994; Thomas et al., 1996; Thomas, Gapais, et al., 1994; Vlasov et al., 1991). The wide central-southern part of the Tajik FTB hosts westward-convex folds and thrusts, grouped into synclinoria and anticlinoria. From the foreland to hinterland, these are Surkhan-darya synclinorium, Kafirnigan anticlinorium, Yavan synclinorium, Vakhsh anticlinorium, and Kulyab synclinorium (Figure 2a). The zonation is less distinct in the southern Tajik FTB due to the forking and waning of the Kafirnigan and Vakhsh anticlinoria. The Kafirnigan anticlinorium abuts in the north against the Ilyak fault, a steep, seismically active (Kufner et al., 2018), composite thin- and thick-skinned structure that accommodates the northeastward decreasing width of the thin-skinned system (Figures 1b and 2a). The Dushanbe trough north of the Ilyak fault represents the only part of the Tajik basin preserved in situ, that is, not involved into the Tajik FTB. The internal Vakhsh anticlinorium and Kulyab synclinorium continue into the narrow northeastern Tajik FTB (Peter the 1st Range; Figure 2a). The anticlines gradually emerge and converge to the erosional front of the Tajik FTB. Ultimately, the Tajik FTB reduces to a deeply eroded, narrow strip hosting a limited number of contractional structures. The southern Kulyab synclinorium features salt tectonics, with salt sheets spilling onto Quaternary strata.

The hitherto presented structural interpretations agree on a strong across- and along-strike variation of shallow structural geometries, ranging from flat-ramp thrust sheets to thrust detachment folds, changing vergence, and variable amounts of shortening absorbed by individual structures. The deep subsurface is much less constrained, in particular concerning the involvement of the pre-evaporite basement. Bekker (1996) proposed a purely thin-skinned model with a passive sub-evaporite basement at ~6–12 km b.s.l., constrained by

magnetotelluric and seismic data; he resolved the entire shortening by stacking of the post-evaporite strata. This concept was followed by Burtman (2000). Thomas, Chauvin, et al. (1994), Thomas et al. (1996), and Bourgeois et al. (1997) invoked models that assumed a thick-skinned involvement of the pre-evaporite basement under the Kafirnigan and Vakhsh anticlinoria, including the propagation of some of the basement-involving reverse faults to the surface, hence a partial coupling between the pre- and post-evaporite levels. Chapman et al. (2017) developed a model in which the basement is strongly imbricated along low-angle thrusts, yet there is a complete decoupling between the pre- and post-evaporite levels.

The amount of shortening in the central-southern, wide part of the Tajik FTB was estimated at ~70 to 240 km, depending on the restoration method and cross-section position: Thomas, Gapais, et al. (1994) and Thomas et al. (1996) postulated a systematic northward increase in shortening, Burtman (2000) obtained ~105 km in the south to ~195 km in the north, and Bourgeois et al. (1997) calculated 150–240 km. The narrow northeastern Tajik FTB yielded low minimum shortening estimates: Hamburger et al. (1992) calculated ~15 km but rejected this value as unrealistic and proposed ~60 km, using less conservative geometric solutions. Even the highest values fall short of the ~300-km N-S shortening postulated from offset facies zones in the Cretaceous-lower Cenozoic strata (Burtman, 2000; Burtman & Molnar, 1993). To reconcile these contradicting estimates, Pavlis et al. (1997) postulated syn-tectonic erosion of the deformation front, keeping up with the rate of the Tajik FTB advance. Accordingly, shortening may not be quantifiable in the northeastern Tajik FTB. In addition to ~E-W shortening, the anticlines of the central-southern Tajik FTB have undergone paleomagnetically determined anticlockwise, vertical-axis rotations (e.g., Pozzi & Feinberg, 1991; Thomas, Chauvin, et al., 1994); they decline from 40° to 50° near the Pamir to 0–15° in the Kafirnigan anticlinorium.

The continental nature of its syn-orogenic strata impede biostratigraphic dating of deformation in the Tajik FTB (e.g., Chapman et al., 2019; Dedow et al., 2020; Klocke et al., 2017). An exception is a locality near the edge of the Tian Shan, where combined biostratigraphic and magnetostratigraphic dating yielded ~11 Ma for the base of thick conglomerate units (Forsten & Sharapov, 2000). Chapman et al.'s (2017) pioneering first low-temperature thermochronologic data set—suggesting that basin inversion started at \leq ~17 Ma—is assessed in Abdulhameed et al. (2020), who showed—in accordance with the work of Käßner et al. (2016) and Jepson et al. (2018) in the Tajik Gissar—that the major phase of the Tajik-basin inversion and western Tian Shan shortening commenced at ~12 Ma, synchronous with and triggered by the lithospheric indentation of India into Asia underneath the Pamir (Kufner et al., 2016).

3. Data and Methods

Figure 2b presents our database, that is, the borehole locations, seismic sections, field stations, detailed maps, and positions of cross sections. The surface data comprise Soviet-time, 1:200,000-scale geologic maps (GRI, 1961–1984), our own field data from three campaigns, and Google Earth® imagery. The fieldwork showed that the maps are adequate for the structure and stratigraphy, except for the often selectively plotted bedding dips. Our field data comprise structural measurements and observations of geometric relationships from outcrop to panorama scale.

The borehole database consists of 676 Soviet-time boreholes for which both coordinates and stratigraphy are known. In addition, a number of boreholes with known stratigraphic tops have no coordinates, but their positions can be approximated from their names and the accompanying geologic information. We used two sets of time domain seismic data: An older, partly declassified set comprises 557 km of 2-D lines through the southern and—to a lesser extent—central part of the Tajik basin; a recent, classified set includes ~1,200 km of 2-D lines through the central and northern part of the Tajik basin (Gaġala, 2014). Borehole time-depth data are missing; thus, no quantitative borehole-seismic correlation was possible. We applied a constant velocity of 4,000 m/s whenever seismic horizons needed to be integrated with borehole tops or were used for cross-section construction. This velocity was found a good approximation for the post-Bukhara Fm intervals that comprise most of the post-salt stratigraphic thickness.

The structural interpretation integrates the seismic, borehole, and surface constraints. First, we used a series of representative seismic lines to construct maps that show the base of the Gaurdak Fm evaporites (“base-salt”) and top of the Bukhara Fm (“top-Bukhara”) and to portray the subsurface structural styles. Local cross sections exploit surface data and link key deep boreholes to the surface geology. Then we constructed five

regional cross sections. Their traces cross key structural units and tectonic boundaries of the Tajik FTB and the Gissar and pass close to key data. The base-salt time-grid was stretched to depth using the constant 4,000 m/s velocity and then intersected with the cross-section traces to obtain the base-salt geometry for each of the cross sections. Then we constructed the supra-salt structural geometries using components of the cross-section balancing strategy (e.g., Dahlstrom, 1969; Woodward et al., 1989): dip-domain method, constant-thickness construction for depth exploration of stratigraphy and detection of internal décollements, line-length conservation for competent units, and cutoff match across faults. We calculated the amount of shortening by line-length restoration of the top of the Bukhara Fm, the youngest, basin-wide, nearly synchronous stratigraphic marker. Sub-salt structures are—to a certain extent—illuminated by modern seismicity (Kufner et al., 2018); we projected the hypocenters within a 20-km-wide swath onto the cross sections.

4. Structural Interpretation

4.1. Basement of the Tajik Basin

Herein, “basement of the Tajik basin” refers to a mechanical basement, that is, the base-salt. The crystalline basement proper is deeper, but the underconstrained thickness of the pre-salt strata (?Triassic-Oxfordian) prohibits precise estimates. The pre-Mesozoic crystalline basement rocks in the Gissar and the northwestern Pamir comprise mostly low-grade Paleozoic sedimentary and volcanic rocks, and voluminous granitoids (Vlasov et al., 1991).

The base-salt of the Tajik basin has not been reached by boreholes except in its very northern part, the Dushanbe trough. The base-salt map in Figure 4 is in the time domain and relies entirely on 2-D seismic interpretation. The base-salt occurs between 0- and 4,750-ms TWT (datum is the sea level), in general deepening southward. The basement of the Tajik Gissar descends steeply in the northern part of the Tajik basin. A 4,750-ms TWT low of the base-salt occurs in the southeastern Tajik basin where it underlies a modern depocenter with a thick Quaternary cover (Figure 4). The northern limit of this basement low is defined by a major, ~NW striking step marked A in Figure 4a. This basement step coincides with a zone where the ~N trending anticlines—outcropping in the north—plunge south below the Quaternary strata (Figure 4b). The 2,500- to 2,750-ms TWT basement culminations B and D are separated by the 3,750-ms TWT depression C. These features correlate roughly with surface geology: Culminations B and D are overlain by the stacked thrust sheets of the Vakhsh and Kafirnigan anticlinoria, respectively, carrying Cretaceous-Paleogene stratigraphy, while depression C underlies the broad Yavan synclinorium filled with thick foreland-basin strata (Figure 4b). The arcuate basement culmination B is the most prominent feature, intersected by multiple seismic lines. Given its position below stacked pre-foreland-basin strata, it may be a velocity pull-up. On the other hand, it is slightly oblique to the surface tectonic trends and coincides with a distinct cluster of seismicity, suggesting a tectonic origin.

The pre-Upper Jurassic basement crops out in the Tajik and Uzbek Gissar (Figure 2a) at elevations of up to 3,000–4,000 m while in the Tajik basin, it is traced seismically at 0- to 4,750-ms TWT. This indicates >12 km of structural relief between the Tajik basin and the Gissar. The Neogene structural fabric of the Tajik Gissar is formed by ~E trending fault zones that splay into a ~NE trending contractional horsetail pattern in the Uzbek Gissar (Figures 1b and 2a). The marginal and internal faults of the Tajik Gissar dip steeply and have dextral-transpressive kinematics (Käbner et al., 2016), locally with remnants of a Triassic-Neogene sedimentary cover preserved in synclines. The Uzbek Gissar consists of three to five basement-rooted thrust sheets, bivergently thrust over the Tajik and Amu Darya basins, yielding a pop-up geometry that is asymmetric with SE vergent thrusting prevailing.

We studied the eastern front of the Uzbek Gissar along three profiles (Figure 5). The most complete one follows the Sangardak-river valley that dissects three successive thrust sheets (Figure 5, section A). The front-most Sangardak anticline is mostly buried under foreland strata, but its presence and geometry are outlined by dip data and outcrops of the early foreland-basin Baljuvon Fm strata in its crestal domain. In addition, a borehole penetrated a subhorizontal Paleogene-Upper Jurassic section, terminating at 3,526 m below surface in the pre-evaporite Oxfordian-Kimmeridgian Kugitang Fm. Neither its name nor its coordinates are known, but accompanying geographic information positions it in the direct proximity of section A (Figure 5). Extrapolation of the surface geometries, using the combined strata thickness from this borehole and the

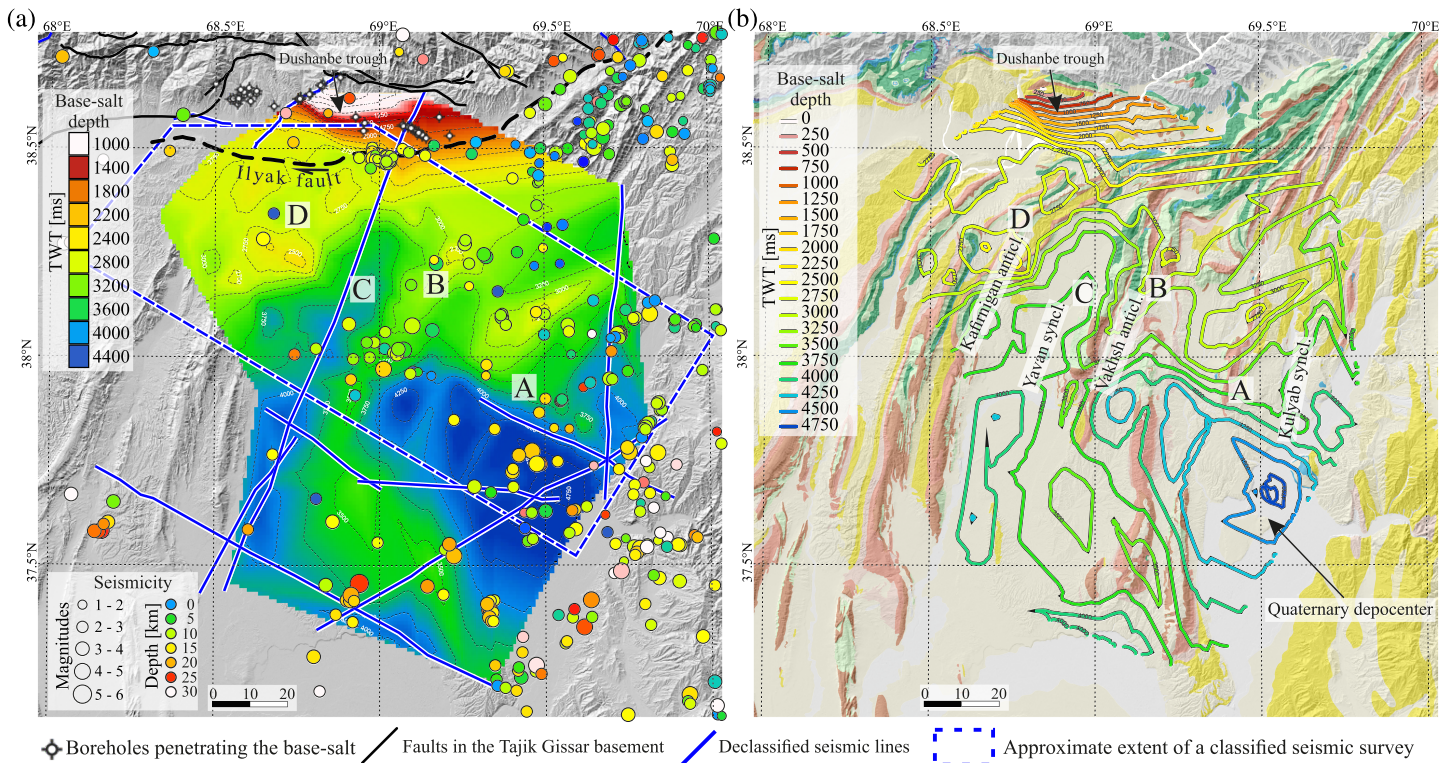


Figure 4. Base-salt map of the central part of the Tajik basin from seismic section interpretation. Figure 2b for location of the map. (a) Base-salt grid with superposed seismicity data from Kufner et al. (2018). (b) Base-salt contours superposed onto the surface geology.

more internal Uzbek Gissar anticlines, places the base-salt culmination at $\sim 3,200$ m b.s.l.; this is $\sim 6,000$ m shallower than in the adjacent Tajik basin. This estimate is a rough approximation due to the lack of subsurface data in the Surkhan-darya synclinorium to its east (Figure 2b). The Sangardak anticline

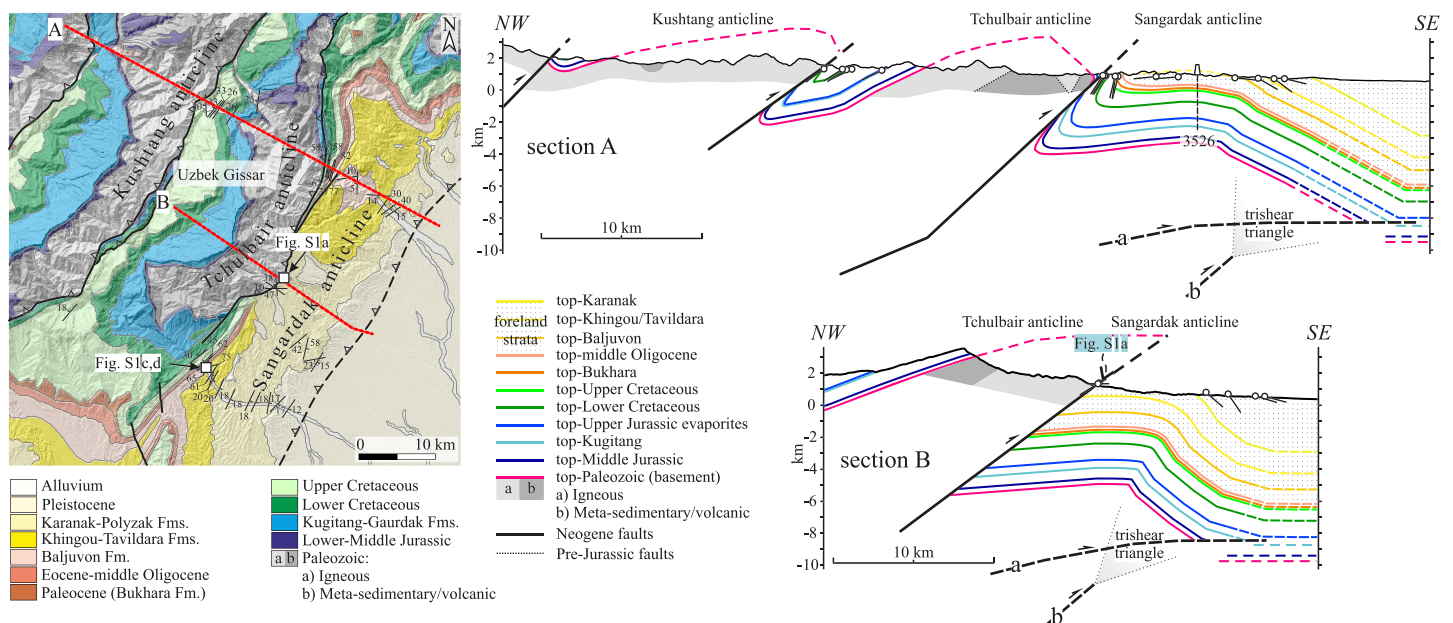


Figure 5. Map of and cross sections through the eastern margin of the Uzbek Gissar. Figure 2b for location of the map.

plunges southwest: The base-salt culmination is at ~4,800 m b.s.l. in the Chinar profile (Figure 5, section B), ~17 km southwest of the Sangardak valley. The emplacement mode of the Sangardak anticline over the Tajik basin is unconstrained, in particular whether its basal thrust breaches out of the basement and flattens into the Upper Jurassic detachment of the Tajik FTB or remains blind. Both possibilities, marked “a” and “b,” respectively, are depicted in cross-sections A and B.

The more internal Tchulbair anticline brings the pre-Jurassic basement to the surface. It has a long and planar backlimb and a short forelimb. The basal thrust of the Tchulbair anticline crops out in the Sangardak profile but has a limited stratigraphic separation: The hanging-wall forelimb passes into an overturned footwall syncline with only the Kugitang Fm missing in the outcrops (Figure 5, section A). The remaining profile—thinned due to forelimb stretching—is complete. This indicates that part of the slip is dissipated by folding of the basement rocks—mainly layered/foliated, low-grade metamorphic schist and limestone. In contrast, in the more southern Chinar profile, the Tchulbair anticline shows a prominent basal thrust, emplacing crystalline rocks onto subhorizontal foreland strata of the Karanak Fm (Figure 5, section B; Figure S1a). The thrust dips ~30°, and a footwall syncline is missing. The hanging wall consists of competent granitoids. This likely explains the lateral change in slip-dissipation mode with respect to the Sangardak profile. We infer similar low climb angles of the main thrusts from low dips of overturned limbs of footwall synclines also elsewhere in the Uzbek Gissar (Figure S1b). A prominent unconformity at the base of the Khingou Fm (about Miocene) occurs in the footwall of the Tchulbair anticline (Figures S1c and S1d). The unconformity passes laterally to parallel geometries; hence, it is progressive. This is the only stratigraphic evidence that permits dating the onset of structural growth in the Uzbek Gissar.

4.2. Ilyak Fault and Dushanbe Trough

The Ilyak fault is a prominent geologic, morphologic, and seismogenic feature (Figure 1b). It accommodates the westward increase in the width of the Tajik FTB and acts as its fold belt-scale lateral ramp. In addition, it delimits the Dushanbe trough—a portion of the Tajik basin preserved in situ between the Tajik FTB in the south and the Tajik Gissar in the north. The Dushanbe trough deepens toward the Ilyak fault (Figure 6, seismic lines A and B). The N to S structural relief at the top-Bukhara level is ~5 km. A dense borehole coverage and the seismic lines reveal basement highs, superposed onto the general deepening trend. These highs parallel the edge of the Tajik Gissar and imply that its thick-skinned structural fabric continues southward. For example, the densely drilled Andygen anticline involves both cover and basement without any major decoupling across the Upper Jurassic layers (Figure 6, seismic line B). Käßner et al. (2016) explained similar yet outcropping structural geometries in the Tajik Gissar by reactivation of basement faults and the strike-slip component of bulk transpression. The Upper Jurassic strata in the Dushanbe trough and the adjacent Tajik Gissar thin toward north; clear evidence for evaporites is missing.

The Ilyak fault acts as a thin-skinned lateral ramp in the post-Jurassic strata. The folds and thrust sheets of the Tajik FTB that abut on the Ilyak fault show a prominent, eastward increasing bending toward the fault zone (Figures 2a and 6). This pattern indicates accumulation of dextral movements. The main cluster of seismicity is located within the pre-Jurassic basement, where it defines a narrow, subvertical zone (Figure 6, seismic line B). The earthquake focal mechanisms change from E to W from prevailing thrusting to dominant dextral strike slip (Figure 6; Figure 5 of Kufner et al., 2018). The superposition of the surface geometries and the deep seismicity indicates a composite character of the ~E striking segment of the Ilyak fault: A thin-skinned lateral ramp overlies an active subvertical basement fault. Despite the intense intra-basement seismic activity, no basement relief is detectable across the Ilyak fault where it is covered by the base-salt map (Figure 4). Although only one seismic line crosses the fault (Figure 6, seismic line B), the top-Bukhara geometry—also constrained by the rich borehole data set in the Dushanbe trough—seems to prolong the northward-rising trend in the synclines of the Tajik FTB in the south. The regional structural relief is thus not affected by the Ilyak fault, further corroborating its strike-slip kinematics. However, the thickness of the Jurassic strata changes across the Ilyak fault (Figure 6, seismic line B). The numerous boreholes drilled into the Andygen anticline north of the Ilyak fault penetrated 200–300 m of undifferentiated Jurassic strata on top of Paleozoic basement. In contrast, the seismic data indicate as much as ~0.5-s TWT (1.0–1.5 km) of Upper Jurassic evaporites in the Yavan synclinorium south of the Ilyak fault. Whether this thickness change occurs just at the Ilyak fault or is distributed over a broader area is uncertain. In either case, the present southern slope of the Tajik Gissar seems to be inherited from a flank of a Jurassic basin. This may

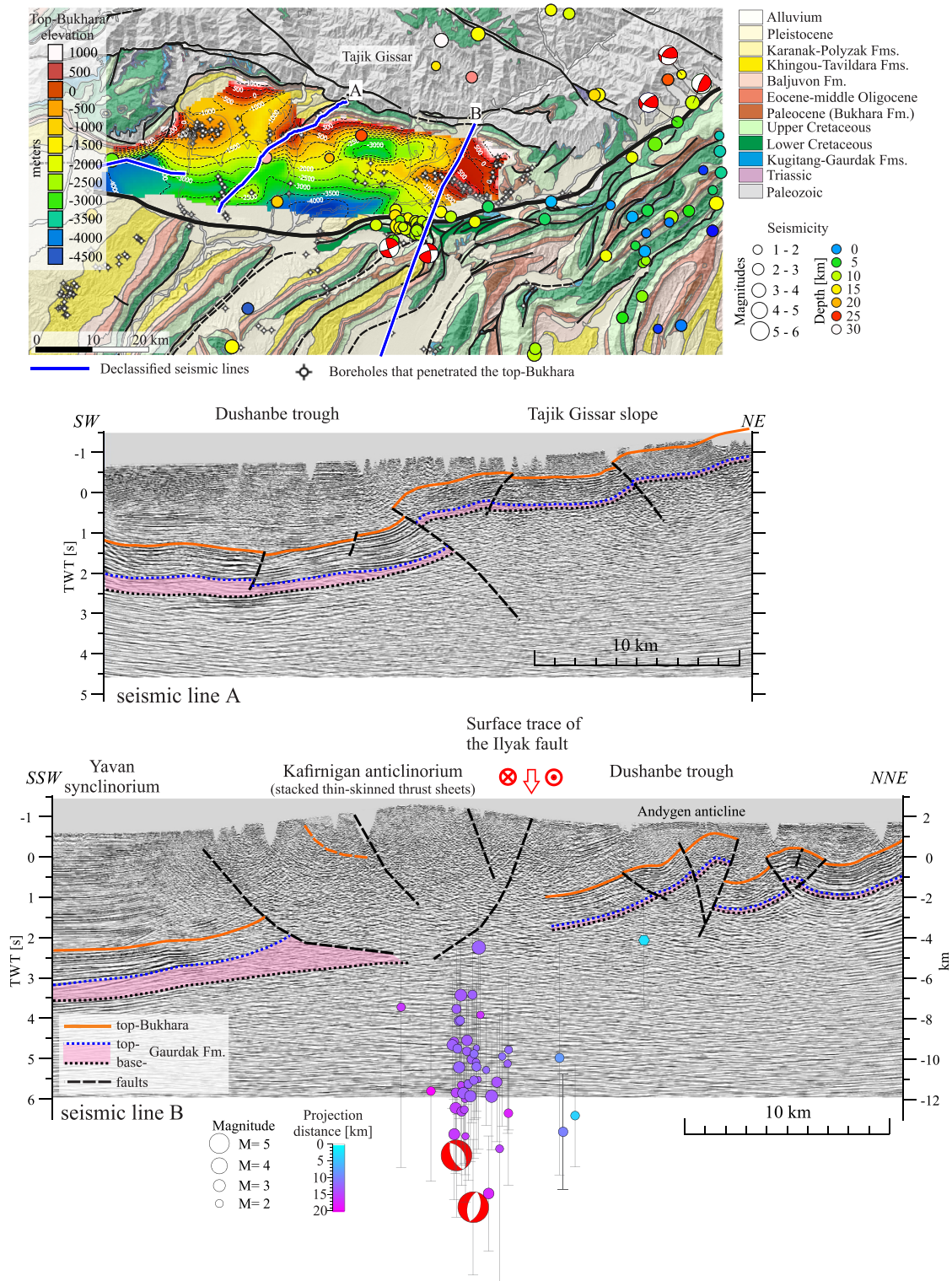


Figure 6. Subsurface constraints on the geometry and kinematics of the Ilyak fault zone and Dushanbe trough. The top-Bukhara map at the top is gridded from boreholes, seismic lines (assumed constant velocity 4,000 m/s), and a classified source for the deepest depressions. Seismicity and earthquake focal mechanisms are from Kufner et al. (2018). Seismic line A crosses the southern slope of the Tajik Gissar and Dushanbe trough. Seismic line B crosses the southern slope of the Tajik Gissar, the Dushanbe trough, the Ilyak fault zone, and the adjacent part of the Tajik fold-and-thrust belt. Left vertical scale (in TWT) refers to the seismic, right vertical scale (in depth) to the seismicity. These are scaled 1:2 (seismic velocity 4,000 m/s). Coplanar structure of the pre-Jurassic basement and post-Jurassic cover in the Dushanbe trough proves thick-skinned tectonics. Concentration of seismicity below the basal detachment of the Tajik fold-and-thrust belt indicates a composite, thin- and thick-skinned nature of the Ilyak fault. The focal mechanisms are shown in cross-sectional view. Figure 2b for location of the map.

explain the superposition of the thin- and thick-skinned segments of the Ilyak fault: The former appears to be controlled by a pinch-out of the Upper Jurassic evaporites, and the latter by a preexisting basement structure.

4.3. Central-Southern Part of the Tajik Fold-and-Thrust Belt

The central-southern, wide part of the Tajik FTB features two imbricate stacks—the Kafirnigan and Vakhsh anticlinoria—facing each other across a common footwall syncline, the Yavan synclinorium. This zonation is prominent in the north, illustrated by a line drawing of a classified seismic line (Figure 7a; Gaġala, 2014). There, seismically resolved displacements of oppositely vergent thrusts, converging toward the Yavan synclinorium, exceed 10 km. Farther south, this pattern becomes progressively less discernible (Figure 7b). The Kafirnigan and Vakhsh anticlinoria lose their amplitudes and coalesce with the Yavan synclinorium to form a train of regularly spaced, upright, round-crested detachment anticlines with no preferred vergence. Fold wavelengths span 11–27 km—typically 15–20 km. The anticline flanks are thrust, and these appear in oppositely vergent pairs, forming U-shaped thrust sheets (Figure 7b; e.g., between 5–25 km and 55–75 km). Individual thrust displacements are ~5 km, exceptionally ~10 km. The base-salt in both seismic lines is deep and appears little deformed.

Within this first-order pattern, the central-southern Tajik FTB hosts a wealth of structural styles changing across and along strike. The northern Kafirnigan anticlinorium features ~ESE vergent thrust sheets, stacked along flat-ramp thrusts; the cross section of Figure 8a—connecting boreholes—offers insight into the subsurface geometries. Wells Kurgancha Severnaya 20 and 21 penetrated the Babatag thrust sheet and pierced its sole thrust ~15 km downdip from its surface trace. Both wells entered the Neogene strata of the structurally lower Karchitau thrust sheet. The total displacement of the Babatag thrust sheet exceeds 15 km, as its footwall continues farther WNW from the two boreholes. Borehole Gardyanushti 1 penetrated the flat-lying Rengan thrust sheet and terminated in the Eocene-Oligocene series of the structurally lower Dagana Kiik thrust sheet (Figure 8a). The sole thrust of the Rengan thrust sheet was pierced ~9 km downdip from its surface trace. Wells Fatrabad 684, 685, and 686 drilled this thrust in a more frontal position; the thrust plane is exposed a few kilometers from the cross-section line. These boreholes and surface ties prove an emplacement of the Rengan thrust sheet over the Dagana Kiik thrust sheet over a distance of ~20 km.

The southern Kafirnigan anticlinorium features thrust detachment folds with thick evaporite cores. As an example, boreholes Tuyuntau 1 and 2 pierced the respectively ~2,000-m and ~3,000-m-thick evaporite core of the Tuyuntau anticline (Figure 8b). The former terminated in the evaporites, and the latter reached a thrust plane and Lower Cretaceous strata in the footwall at ~5,500 m below surface; the thrust displacement is ~5 km. Importantly, the Tuyuntau anticline is the southern extension of the Babatag thrust sheet that has >15 km of displacement (Figure 8a). Hence, in addition to the N to S change in structural style, the boreholes testify to a N to S decrease of displacement, in agreement with the seismic data (Figure 7).

The Yavan synclinorium in the footwall of the Kafirnigan anticlinorium is narrow in the north and widens southward (Figure 9). A dense borehole coverage permits tracing of the main anticlines, while seismic lines resolve synclines. The along-strike seismic line A (Figure 9) cuts all major anticlinal trends of the Yavan synclinorium, providing insight into the depths to the top-Bukhara and the base-salt. The minimum synclinorium depth is calibrated by the Yavan 1 borehole that pierced 5,040 m of strata without reaching the Bukhara Fm (Figure 9 for borehole position). The post-salt formations are nearly flat and undeformed in the north. Buried anticlines appear in the southern part of the synclinorium. These are continuations of the main thrust sheets and anticlines exposed in the surrounding anticlinoria but with lower amplitudes and displacements. For example, the Karatau uprooted anticline of the Vakhsh anticlinorium (see next paragraph) transitions southward into the buried, weakly W vergent Akbash detachment anticline in the Yavan synclinorium (Figure 9, seismic line B). Likewise, the outcropping Dagana Kiik anticline of the Kafirnigan anticlinorium continues into the buried Karadum anticline in the Yavan synclinorium. In the extreme south of the Tajik FTB, the Yavan synclinorium cannot be separated from the adjacent Kafirnigan and Vakhsh anticlinoria (Figure 7b).

The Vakhsh anticlinorium displays similar along-strike structural variations as the Kafirnigan anticlinorium, expressed in progressively less tectonic stacking and decreasing amount of exhumation from N to S. The most elevated part of the Vakhsh anticlinorium consists of three anticlines—Karatau, Sarsaryak, and

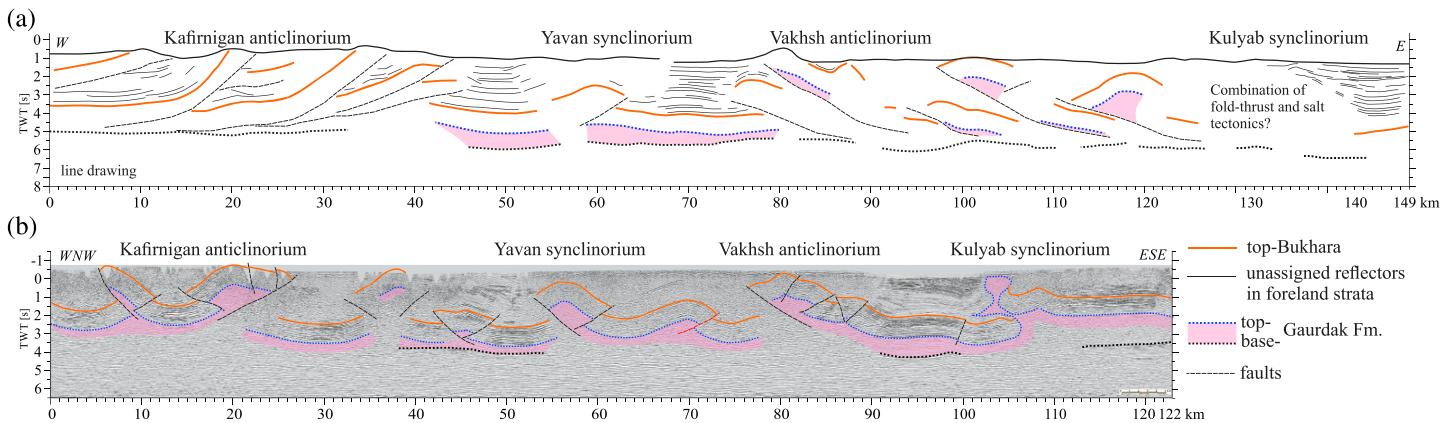


Figure 7. Structural styles of the central and southern parts of the Tajik fold-and-thrust belt (FTB) in regional seismic lines (Gagała, 2014). (a) Line drawing of a classified seismic line depicting a general bivergent and convergent geometry of the Tajik FTB south of the Ilyak fault zone. The seismic is located inside the polygon labeled “Approximate extent of a classified 2-D seismic survey” in Figure 2b. (b) Seismic line across the southern Tajik FTB, depicting regularly spaced, thrust detachment folds over a little deformed basement. Figure 2b for location of the seismic line.

Sanglak—detached along the Upper Jurassic evaporites (Figure 10a). These three main anticlines are tightly stacked, forming a topographic obstacle for the course of the Vakhsh river. A series of narrower anticlines—Tabakchin, Donguztyube, and Aksuyak—is detached along shallower horizons, unusual for the Tajik FTB. Surface data and boreholes Yavan 1 and Sanglak 1S permit the construction of a high-resolution section across this part of the Vakhsh anticlinorium (Figure 10a). Borehole Yavan 1 constrains the footwall depth of the entire thrust stack. The most external of the exposed structures—the Karatau anticline—has a round hinge passing into a backlimb dipping 65–70°E. The structurally higher Sarsaryak anticline has the geometry of a homoclinal thrust sheet dipping ~43°E, likely mimicking the dip of the basal thrust. The anticline continues to the S across a relay zone as the Tchaltau anticline (Figure 10a). The northern termination of the Sarsaryak anticline is defined by a lateral ramp across which the sole thrust climbs up into the Upper Cretaceous; there, Jurassic evaporites form a body with lateral contacts against Lower Cretaceous-Neogene strata. The basal thrust of the Sarsaryak anticline cuts down-section into the steep backlimb of the Karatau anticline (generalized dip marks in the geologic map in Figures 10a and S3). This

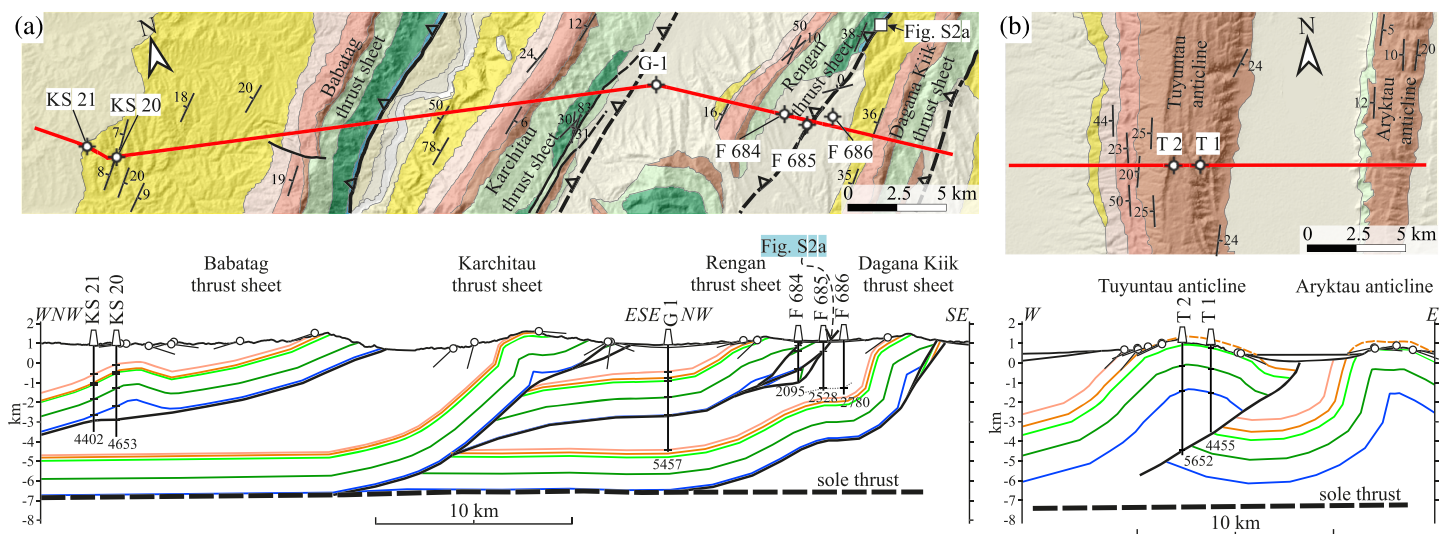


Figure 8. Surface and borehole constraints on the geometry of the Kafirnigan anticlinorium. Legend as in Figure 6. (a) Cross section through a line of deep boreholes reveals a long-distance stacking along ~E vergent thrusts in the northern Kafirnigan anticlinorium. Boreholes: KS = Kurgancha Severnaya; G = Gardyanushti; F = Fatrabat. (b) Section across the Tuyuntau anticline in the southern Kafirnigan anticlinorium based on boreholes Tuyuntau 1 and 2. Figure 2b for location of the maps.

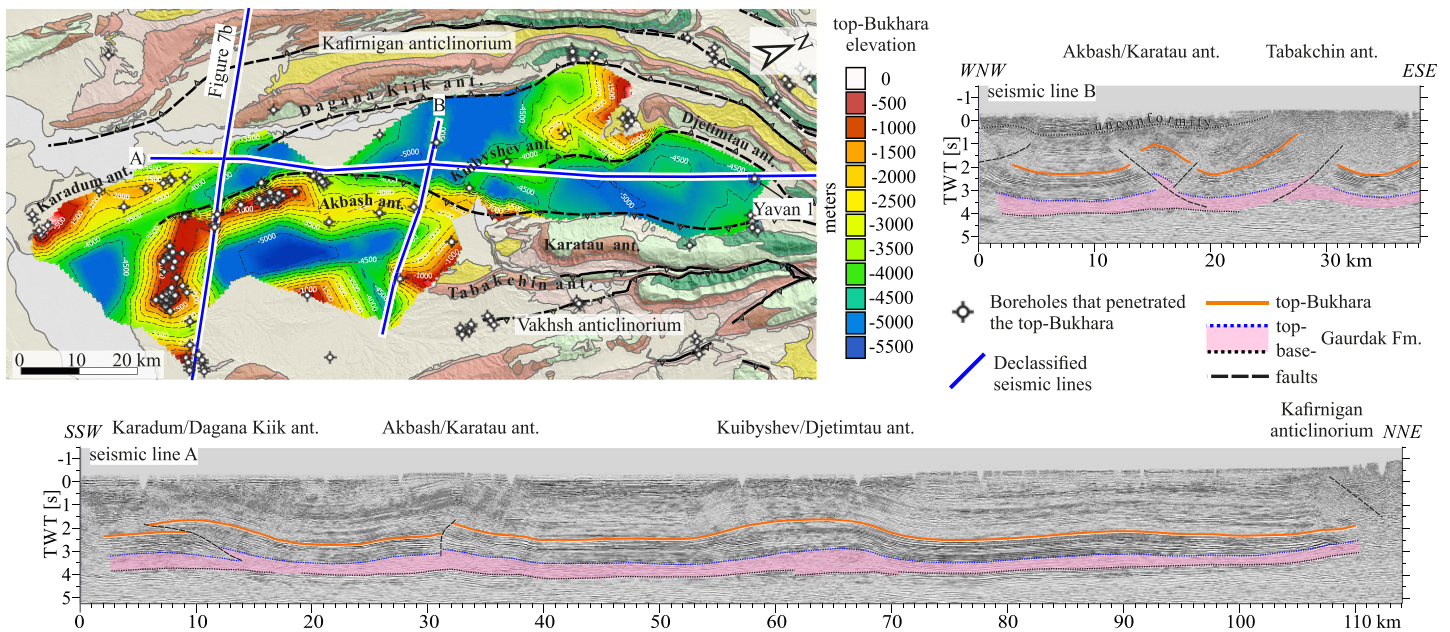


Figure 9. Borehole and seismic constraints on the depth and internal structures of the Yavan synclinorium. The top-Bukhara map is gridded from boreholes, seismic lines (assumed constant velocity 4,000 m/s), and a classified source for the deepest depressions. Legend for the geologic map as in Figure 6, for the seismic lines as in Figure 7. Longitudinal seismic line A along the Yavan synclinorium crosses or passes close to the main anticlines. The top-basement is deep and flat all along the Yavan synclinorium. Seismic line B crosses the Akbash anticline (continuation of the outcropping Karatau anticline). The line shows a moderately developed, thrusted detachment anticline topped by a syn- to post-kinematic unconformity, which remains undated due to the lack of stratigraphic information in the foreland-basin section. Figure 2b for location of the map.

break-back thrust propagation is also evidenced by well Sanglak 1S (Figure 10a, cross section); it penetrated foreland clastic rocks of the Baljuvon Fm below the basal thrust of the Sanglak anticline, while a footwall cutoff of the base of the Baljuvon Fm is exposed in a more updip position. We interpret the round Karatau anticline and the Sanglak box-anticline as uprooted detachment folds transported along low-angle thrusts with kilometeric displacements.

Thrust displacements diminish southward, and geometries change from stacked thrust sheets to thrusted detachment folds with thick salt cores. As an example, a series of boreholes penetrated the Karatau-South anticline (Figure 10b, location see Figure 2b). Deep well Karatau Yuzhnaya 1 penetrated >3 km of Gaurdak Fm evaporites in the core of the anticline, pierced a thrust at 5,800 m below the surface, and entered Lower Cretaceous strata in the footwall. Shallow well Karatau Yuzhnaya 8 constrains this thrust in a frontal position. Well Karatau Yuzhnaya 3 drilled the backlimb, penetrating >4,000 m of steeply dipping Paleogene-Cretaceous strata. These wells in combination with the surface data define the Karatau-South anticline as an uprooted detachment fold, displaced ~4 km to the west.

The Kulyab synclinorium—the most internal structural domain adjacent to the Pamir—exposes successive anticlines at progressively shallower levels, and synclines contain progressively more complete foreland-basin stratigraphic sections from W to E. Surface structural styles are sharp-crested anticlines and deep, symmetric synclines. The foreland-basin strata in the synclines dip up to ~70°. Interlimb angles of <70° suggest decoupling in the anticlinal cores along one or more internal décollements, like those we observed in the Upper Cretaceous-Paleogene layers of the Vakhsh anticlinorium. A depocenter with >1,200 m of Quaternary strata exists in the southern Kulyab synclinorium (Figures 2a and 4b).

The Kulyab synclinorium evidences active salt tectonics. The surface expression of ongoing halokinesis are salt fountains and sheets. Their extents are delineated by outcrops, morphology, and 66 wells that drilled Upper Jurassic salt in allochthonous positions (Figure 11). Four structures of this type have been identified at various stages of degradation. The Hoja Mumin salt sheet is active and shows a typical salt-fountain morphology (Figure S4a). It has a pronounced dynamic bulge and relatively thin salt glaciers advancing over the modern topography (Figure S4b). The rate of salt supply outcompetes the rate of gravitational spreading, and

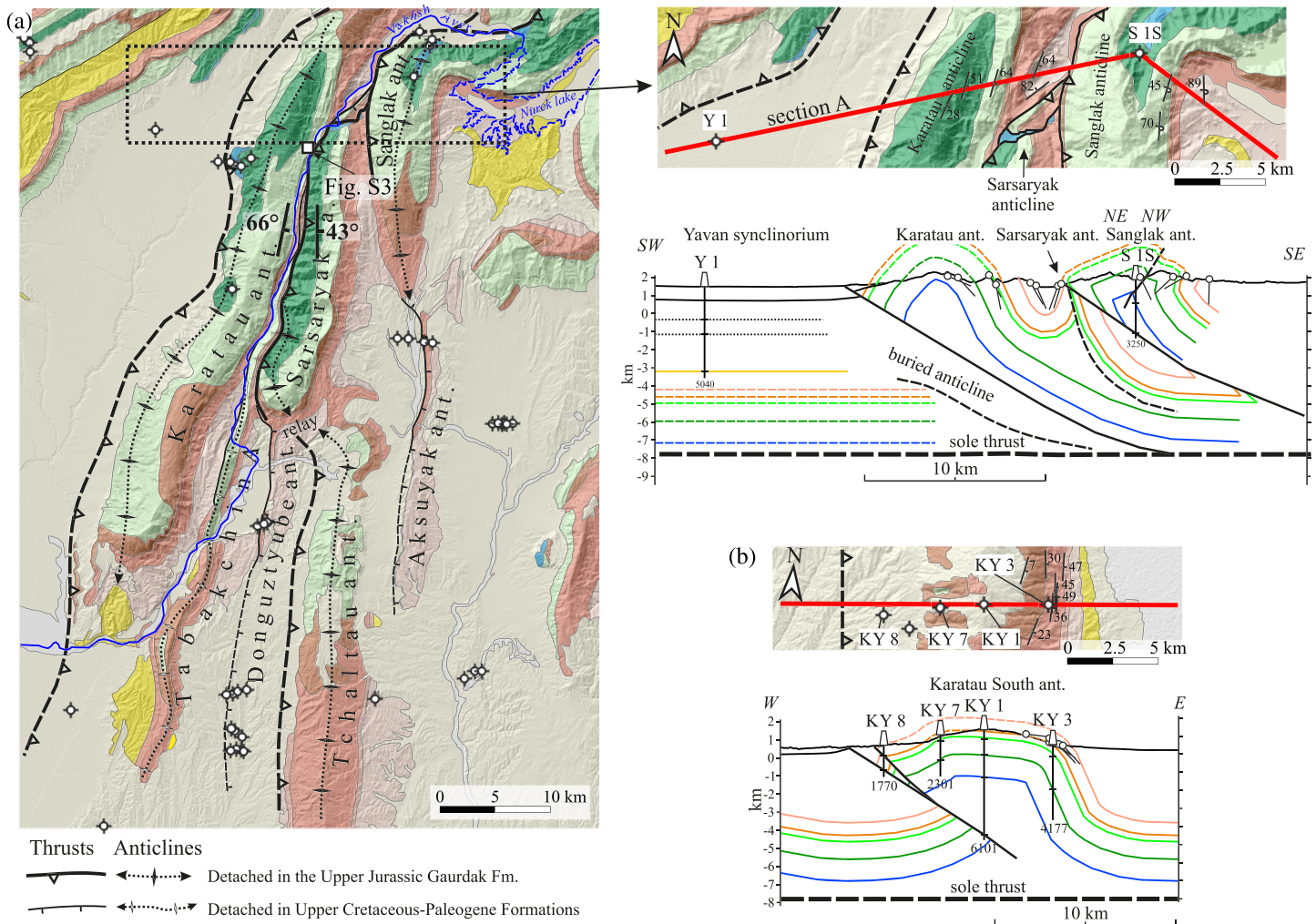


Figure 10. Surface and borehole constraints on the geometry of the Vakhsh anticlinorium. (a) Geologic map reveals two families of anticlines: The main ones are detached along the Upper Jurassic Gaurdak Fm evaporites and the short-wavelength ones along Upper Cretaceous-Paleogene strata. Legends as in Figure 6 (maps) and Figure 5 (cross sections). Cross section connects the Yavan 1 and Sanglak 1S boreholes, showing thrusting of the Vakhsh anticlinorium thrust stack over the Yavan synclinorium. The thick salt cores of the Karatau and Sanglak anticlines point at detachment folding prior to thrusting. The sole thrust of the Sanglak anticline cuts down-section into the lateral termination of the Sarsaryak anticline, indicating a break-back thrusting succession (cf. Figure S3). (b) Section across the Karatau-South anticline based on boreholes Karatau Yuzhnaya 1, 3, 7, and 8. Figure 2b for location of the map.

a salt source must still be thriving at depth. The salt thickness is not well constrained as only one borehole was drilled through the salt in a peripheral position. The Hoja Sartis salt sheet is probably inactive; it has a prominent topographic expression but a flat top, thick edges, and a strongly karstified surface. Its salt supply is likely exhausted, and the sheet is in a phase of lateral spreading. The boreholes proved a salt thickness of up to 2,000 m. The Tanapchi salt sheet is inactive. It has a thick veneer of Quaternary sediments on top, and a portion of the original thickness was lost to erosion and dissolution. The maximum salt thickness in the boreholes is 1,250 m. The Alimtau salt sheet is inactive and entirely buried under Quaternary-Recent strata. It is the spatially most extensive sheet, but its outline is visible only in remote-sensing data sets, for example, the slope map of Figure 11. Given its large size and morphology, it is possibly a salt canopy associated with three feeders. The thickest salt documented by boreholes is 1,240 m. In addition to the salt sheets, a salt plug (Figure S4c; P in Figure 11) occurs along the frontal thrust of the Dzhilanytau anticline. This may represent the youngest and yet developing salt extrusion in this area.

The Hoja Sartis salt sheet originates from the Pushion anticline. Both structures are thoroughly covered by borehole data. The Pushion anticline has a Q-tip (cotton-swab) geometry with the Hoja Sartis salt sheet at its southern tip, a remnant salt diapir at its northern tip, and a fault in between (Figure 12a). We interpret

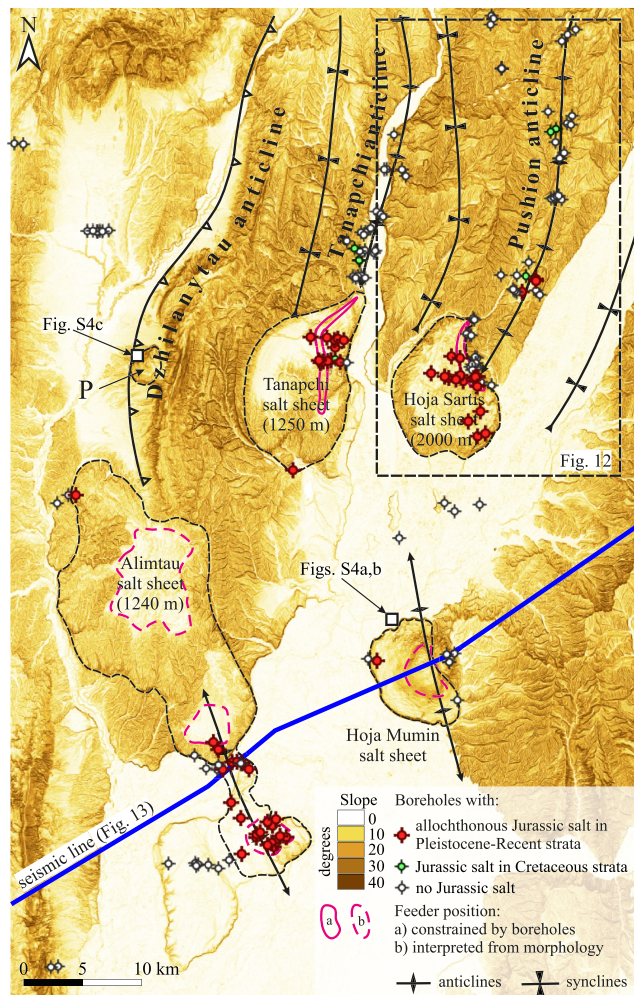


Figure 11. Slope map of the southern Kulyab synclinorium derived from a 30×30 DEM ALOS data set emphasizing outlines of exposed or near-surface salt sheets. Numbers below salt sheet names represent the highest thickness of allochthonous Late Jurassic salt penetrated by boreholes.

this fault as a weld, although poor exposure prohibits direct observations. The Hoja Sartis salt sheet was drilled by 34 boreholes; 16 have stratigraphic logs (Figures 12a–12c). The base of the salt sheet was reached by 12 holes, 4 terminated in the salt. The boreholes proved Quaternary strata or an unconformity below the salt, providing the age of sheet advance. Figures 12b and 12c show base-salt and salt isopach maps. The latter omits the Holocene residua on top of the salt sheet and the ancient residua embedded in the salt and drilled by some wells. The salt volume is $\sim 46 \text{ km}^3$. The Hoja Sartis salt sheet is highly asymmetric, being thickest at its eastern edge, where the base-salt descends below 1,100 m b.s.l. (Figure 12b) and the salt is 2,000 m thick (Figure 12c). We interpret this asymmetry to reflect the feeder position. The cross section through the salt sheet and its western envelope (Figure 12d) is based on a line of wells: It outlines the steep limbs of the Pushion anticline and a feeder in its core. Farther north, another cross section (Kukushkin, unpublished report, 1979) shows a thick layer of Jurassic salt wedged in between Upper Cretaceous Formations beneath the northern flank of the Pushion anticline (Figure 12e). This geometry resembles a salt wing. The Pushion Severnaya 537 well pierced the outcropping fault—here interpreted as a secondary weld—in the subsurface. The combined data imply that the southern Pushion anticline is a squeezed, preexisting diapir; however, some key supporting evidence, for example, halokinetic sequences, is missing.

A seismic line passing through the Hoja Mumin and Alimtau salt sheets crosses the salt-tectonic domain (Figure 13, trace in Figure 11). Seismically well-resolved synclines are separated by poorly imaged anticlines; the salt sheets are located on their tops. Although not fully interpretable due to the seismic quality, the anticlines show features of squeezed salt diapirs. The anticline below the Hoja Mumin salt fountain is possibly an incompletely welded diapir, as reflectors on both sides do not meet except at the deepest level. We interpret the wide zone of seismic noise in between as a remnant diapir (Figure 13, d1). The Hoja Mumin salt fountain is still supplied (note fresh morphology in Figure S4a), favoring an active diapir at depth. Seismic patterns below the Alimtau salt sheet are complex. Given the shallow position of the top-Bukhara and an exhausted salt supply to the Alimtau salt sheet, the feeding diapir may be entirely squeezed out.

Two buried salt bodies (Figure 13, d2 and d3) appear in the seismic line. Their cross-sectional shapes are intermediate between flaring diapirs and salt sheets. The deeper parts of their anticlines and the connection between the diapiric and mother salt are not resolved. Wedge-like disharmony between the foreland-basin strata reflectors—marked as w1 and w2 in Figure 13—may represent salt wings or an older level of salt sheets. The salt accumulations marked as d1, d2, and d3 have tops at a similar position below a major intra-Neogene unconformity and are sealed by the youngest, but stratigraphically undated package of foreland-basin strata. This indicates a phase of accelerated salt expulsion with respect to sedimentation rate, followed by relative quiescence. The first possibly correlates with the main phase of tectonic shortening. The modern salt expulsion likely marks rejuvenated shortening in the southern part of the Tajik FTB. The onset of the primary halokinesis is not directly constrained, as the data do not permit the identification of univocal halokinetic sequences. Short-wavelength structural complications in the Cretaceous-Paleogene strata next to the salt may be considered folded flaps (Figure 12d). This may indicate a Cretaceous onset of halokinesis, but a later trigger due to differential loading by the foreland-basin sediments cannot be ruled out.

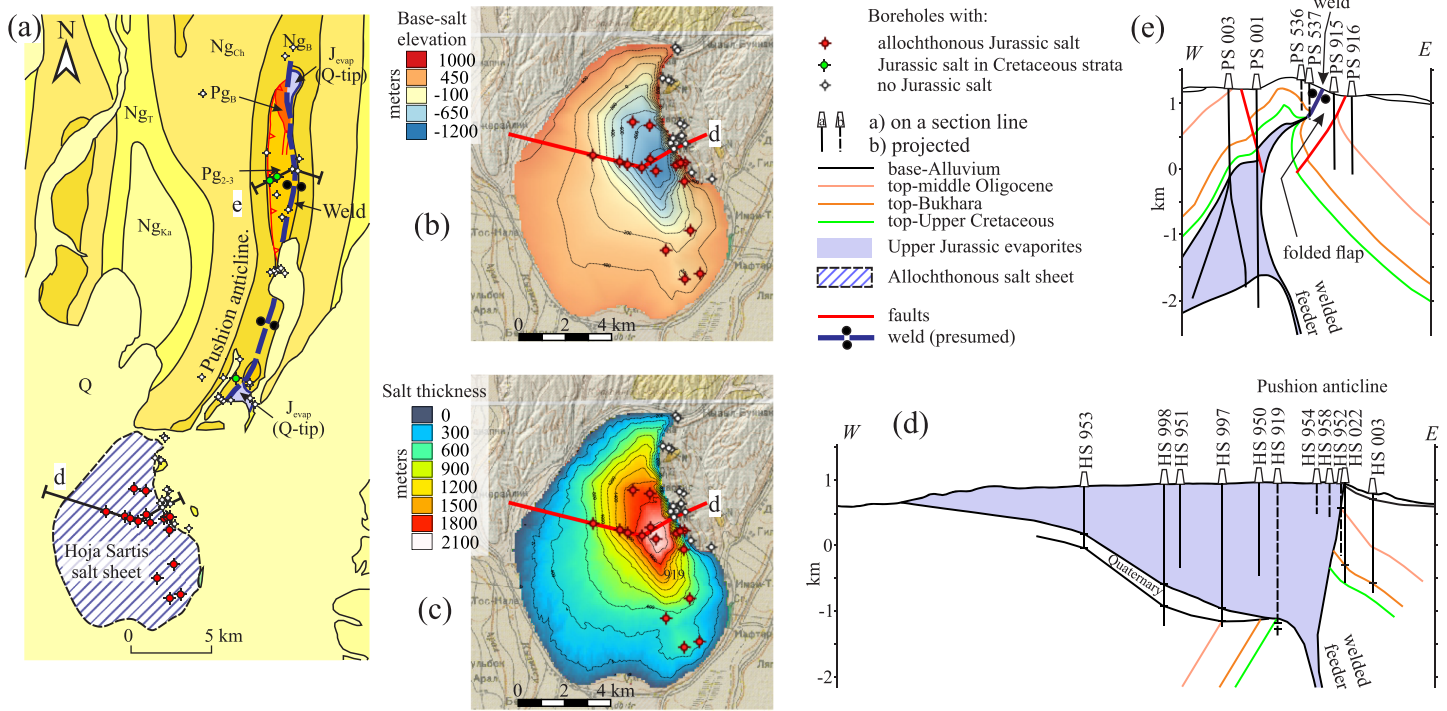


Figure 12. Anatomy of the Pushion anticline and the Hoja Sartis salt sheet. (a) Map showing a Q-tip (cotton-swab) geometry of the Pushion anticline from which the Hoja Sartis salt sheet originates. (b) Base-salt map based on boreholes. (c) Salt isopach map. (d) Cross section through the Hoja Sartis salt sheet. Feeder position is approximated by boreholes (HS = Hoja Sartis). (e) Section across the central segment of the Q-tip geometry based on boreholes (PS = Pushion Severnaya; Kukushkin, unpublished report, 1979). Thick near-surface salt accumulation in the western flank of the Pushion anticline resembles a salt wing.

4.4. Northeastern Tajik Fold-and-Thrust Belt

The Vakhsh anticlinorium and the Kulyab synclinorium continue northeastward into the corridor between the Tian Shan and the Pamir (Figure 2). They merge into a train of anticlines, exposing progressively deeper stratigraphic levels along strike, that is, from SW to NE, and from hinterland to foreland. The individual folds parallel the edge of the Pamir but strike obliquely to the southern margin of the Tian Shan. As a result, successively more internal anticlines approach—and ultimately abut—on the thin-skinned deformation front (Leith & Alvarez, 1985). We studied the structure of the northeastern Tajik FTB along the Obikhingou and Sari-Ob river valleys (“Pamir Highway”). Figure 14 shows a map and two cross sections whose different orientations account for the changing course of the Obikhingou valley with respect to the structural fabric.

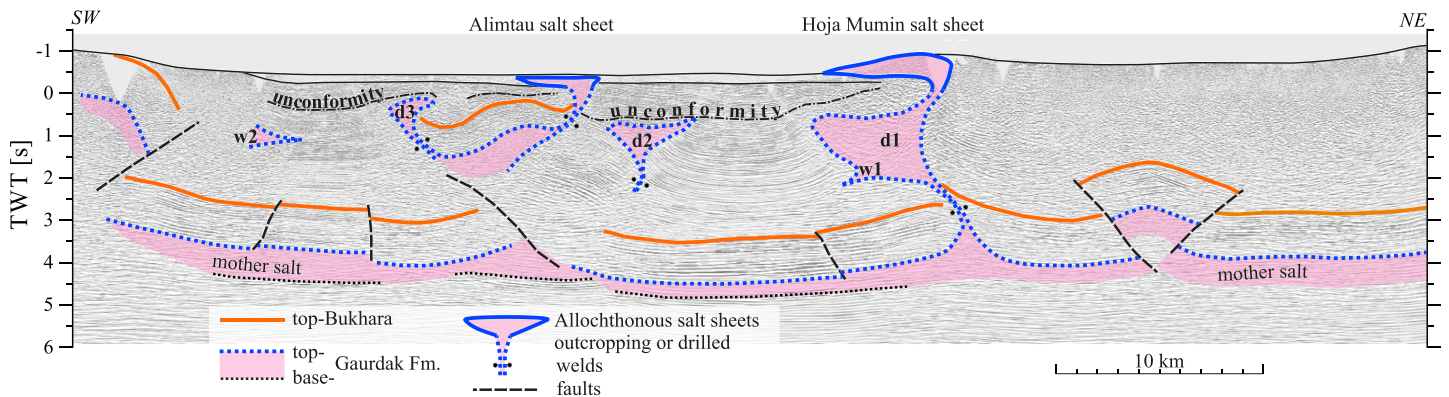


Figure 13. Seismic line across the salt-tectonic domain. Line location is indicated in Figures 2b and 11. Interpreted remnant diapirs marked as d1, d2, and d3. Possible salt wings marked as w1 and w2. Prominent syn-tectonic unconformity remains undated due to the lack of boreholes.

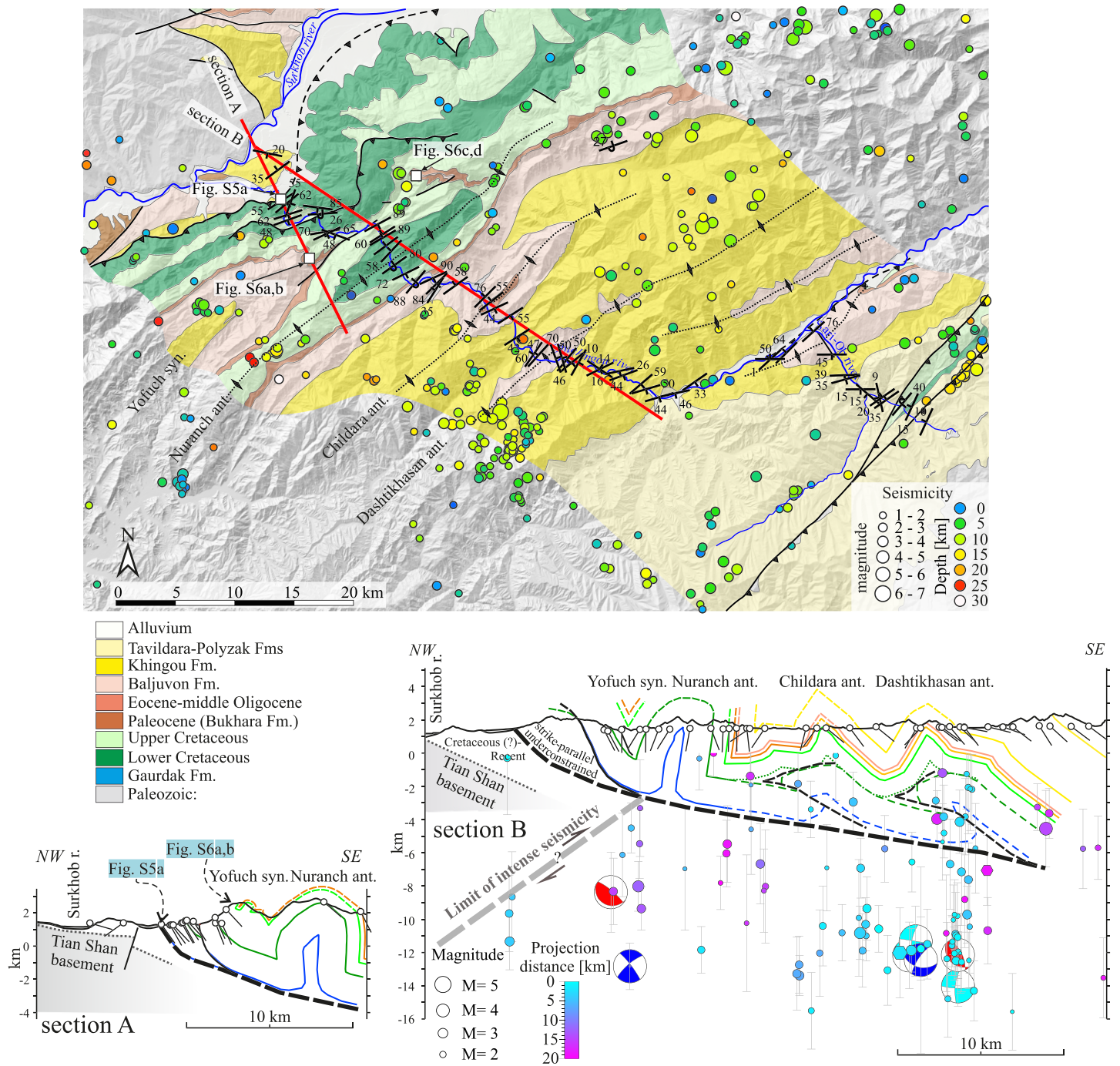


Figure 14. Geologic map and cross sections through the northeastern Tajik fold-and-thrust belt (FTB) along the Obikhingou and Sari-Ob river valleys. The map is based on our field observations, Soviet 1:200,000 maps J-42-11, 17, and bed tracing on top of Google Earth® images. Seismicity and earthquake focal mechanism are from Kufner et al. (2018). Legend for the cross sections as in Figure 5. Section A: front of the Tajik FTB. Section B: section across the Tajik FTB yet with the frontal part less constrained than in section A. Seismicity projected within a 20-km-wide swath on the section trace. Focal mechanisms are cross-sectional projections. Figure 2b for location of the map.

The Tajik FTB is separated from the Tian Shan by the Surkhob-river valley. Its northern bank follows the basement rocks of the Tian Shan with fragmentarily preserved autochthonous Cretaceous-Neogene strata. The Cretaceous-Paleogene section is up to ~700 m thick—the thickness of the Neogene is

unconstrained. Its southern bank erodes the leading edge of the thin-skinned system, exposing up to ~2,400-m-thick Cretaceous-Paleogene strata (cf. Figure 6 of Leith & Alvarez, 1985). The Tajik FTB sole thrust is widely covered by Quaternary gravels and obscured by landslides. It locally overrides modern fluvial deposits, proving active thrusting (Soviet literature summarized in Burtman & Molnar, 1993; Pavlis et al., 1997). On a regional scale, the trace of the frontal thrust is irregular, following embayments and promontories of the Tian Shan margin. The evaporitic sole of the Tajik FTB—dipping up to 55–60°—is exposed where the Obikhingou river dissects the thrust front (cross-section A in Figures 14 and S5a). Its ongoing activity is evidenced by a fault scarp (Figure S5a, Google Earth inset). Even steeper dips of up to ~70° occur farther NE—beyond the map in Figure 14—where the Tajik FTB directly overrides Tian Shan basement rocks (Figure S5b).

The frontal part of the northeastern Tajik FTB exposes stacked anticlines eroded down to the Lower Cretaceous-Paleogene stratigraphic level. In addition to the basal detachment in the Upper Jurassic evaporites, Upper Cretaceous-Paleogene anhydrite-bearing strata acted as a secondary décollement. This is best evidenced by the geometry of the Yofuch syncline. More than 1,500 m of topographic relief between the Obikhingou river bed and the mountain tops offers a 3-D perspective onto the geometry of this syncline. The Yofuch syncline is narrow, nearly isoclinal at the valley bottom, where Lower Cretaceous strata of its subvertical flanks are in direct contact (cross-section A in Figure 14). It opens up upward where tightly folded Upper Cretaceous-Paleogene strata are exposed (cross-section B in Figure 14; Figure S6). The thickness of the folded strata is multiplied with respect to the depositional thickness, indicating an out-of-syncline evacuation of the Upper Cretaceous anhydrite-bearing strata.

The next to the hinterland, and most prominent structure of the Tajik FTB in the studied section, is the Nuranch anticline. It shows an isoclinal geometry with vertical, ~4-km-long flanks, and a narrow core. The Nuranch anticline converges northeastward to a zone of complex deformation at the front of the Tajik FTB, but its vertical or even strongly overturned, SE vergent, southwestern flank can be traced several tens of kilometers northeastward (Figure 2b in Pavlis et al., 1997). The more internal Childara and Dashtikhasan anticlines are eroded down to the top-Upper Cretaceous and the Eocene-Oligocene, respectively. These anticlines have sharp crests and acute interlimb angles (cross-section B in Figure 14). Their tight profiles require an intermediate detachment to account for the space problems below the extrapolated top-Lower Cretaceous (dotted green line in Figure 14c). This décollement is likely in the Upper Cretaceous anhydrite-bearing beds, in accordance with our observations in the core of the Yofuch syncline (Figure S6). We resolve the deeper portions of the anticlines through fish-tail geometries, developed within multilayer detachment folds; this solution—marked with dashed lines in cross-section B (Figure 14)—is conceptual, and more complex geometries are possible (e.g., Butler et al., 2019). The intervening synclines contain progressively more complete sections of the foreland-basin strata toward the hinterland; the innermost syncline—its NE flank is depicted in cross-section B (Figure 14)—hosts a complete foreland-basin section up to the Polyzak Fm.

While the progressively more complete stratigraphy preserved from the foreland to the hinterland indicates a descent of the sole thrust of the Tajik FTB, the footwall of the thin-skinned system remains underconstrained; this refers to the footwall cutoff of the Tajik FTB and the geometry of the pre-Jurassic basement. The former aspect remains open, as the surface geometries do not allow a solution. The distribution of modern seismicity (Kufner et al., 2018) partly illuminates the latter aspect. We projected earthquake hypocenters in a 20-km-wide swath onto the cross-section B of Figure 14. The seismicity concentrates in the sub-detachment basement. Given the depth uncertainties, only a few events can univocally be attributed to the Tajik FTB-internal deformation. Compared to the basement underneath the Tajik FTB, the basement below the Tian Shan margin appears—on first order—aseismic. The focal mechanisms indicate thrusting with a subordinate dextral strike-slip component (Kufner et al., 2018). Although no strong alignments occur, the northeastern limit of the projected earthquakes defines a NE dipping interface (cross-section B, Figure 14, gray dashed line). This may be interpreted as evidence of the Tajik FTB basement being underthrust below the Tian Shan (Figures 2b and 2c of Pavlis et al., 1997). Therefore, the tight stacking and deep erosion along the front of the northeastern Tajik FTB may be the result of the active buttressing of the Tajik FTB by a blind ramp in the Tian Shan and the competition between superposed thin- and thick-skinned thrust systems.

4.5. Hinterland of the Tajik Fold-and-Thrust Belt and the Darvaz Fault Zone

The Darvaz fault zone is considered the main structure accommodating the northward advance of the Pamir with respect to the Tajik basin (e.g., Burtman & Molnar, 1993). It is accessible in the Shurobod area, where the Panj river breaks out of the Pamir (in the south), and along the “Pamir Highway” (in the north; Figure 2b). In both areas, growth synclines filled with foreland-basin strata form the western, down-thrown side of the Darvaz fault. In the Shurobod area, successively older stratigraphic units of the Tajik basin emerge toward the edge of the Pamir (Figure 15a); a complete stratigraphic section—from the Pliocene Polyzak-Karanak Fms down to the Upper Jurassic evaporites—is exposed. The structure is a broad, $\sim 20^\circ$ W dipping homocline with a narrow overturned flank adjacent to the Darvaz fault zone (Figure 15b). Neogene growth strata accommodate a drastic dip change between these two segments (Figure S7a): The growth starts in the middle Khingou Fm and ends in the upper Tavildara Fm along the Kishti poyon profile (Figures 15a and 15b; Dedow et al., 2020). Also along the Shurobod-road profile (Figure 15a), the growth starts in the middle Khingou Fm. The overturned Mesozoic section is separated at the surface from the Pamir basement by a 1- to 3-km-wide and < 80 -km-long structural depression; its boundary faults form the Darvaz fault zone (Figures 15a and 15b). Modern fault scarps (Figure S7b) and the topographic position of the stratigraphic units (Figure S7c) imply a dip-slip component. Although seismic activity along this segment of the Darvaz fault zone is scarce (Figure 15a), focal mechanism from the global CMT database record sinistral strike-slip displacements farther south (Kufner et al., 2018).

The trace of the eastern strand of the Darvaz fault zone is sinuous. A pronounced bend occurs where the Panj river breaks out of the Pamir; there, outcrop-scale, \sim E striking normal faults indicate a releasing step (Figures 15a and S7d), consistent with the overall sinistral kinematics. Locally, transgressive Neogene strata cover the western Pamir basement rocks (Figure 2a; Figure 15a, southeastern corner of the map). They overlie a rugged erosional surface and display growth geometries (Figure S7e; Dedow et al., 2020). A strip of Neogene conglomerates also occurs in the axial graben of the Darvaz fault zone (Figure S7f). Based on their topographic position, these strata correlate with the upper part of the growth strata or the post-growth succession from the adjacent margin of the Tajik basin. They indicate back-stepping of the foreland depositional system onto the hinterland.

The Pamir Highway profile in the north exposes a growth syncline in the down-thrown side of the Darvaz fault (Figures 15c and 15d). Pre-growth Khingou Fm strata are unconformably covered by massive conglomerates of the Tavildara Fm with growth geometries (Figure S8a). The Darvaz fault zone comprises three strands visible in geology and morphology. The northern one separates Khingou Fm strata from an overturned Cretaceous section (Figure S8b); the middle one separates Cretaceous strata of the Tajik basin from Permian limestone of the Pamir; the southern, most internal one cuts through the Paleozoic basement of the Pamir (Figures 15c and 15d). Most of the present 6–8 km of structural relief across the Darvaz fault zone was built before the deposition of the transgressive Neogene conglomerates that conceal much of the hanging-wall architecture (Figure 15d; Klocke et al., 2017). The lack of significant modern vertical offsets, the occurrence of horizontally offset topographic markers (Figure 15c, inset), and the focal-mechanism solutions demonstrate the active, sinistral strike-slip kinematics (e.g., Kuchai & Trifonov, 1977; Kufner et al., 2018; Nikonov, 1975). In contrast to the Shurobod area, the northern Darvaz fault zone has a pronounced seismic expression. The hypocenters occur in two clusters and, if connected, outline a subvertical seismogenic zone descending to ~ 20 km below the surface trace of the Darvaz fault (Figures 15c and 15d).

5. Regional Cross Sections

Five regional cross sections image the Tajik-basin structure (Figure 16). They illustrate a drastic increase of the Tajik FTB width across the Ilyak-fault lateral ramp (section A vs. sections B–E) that is not associated with a significant difference in the amount of internal folding and thrust stacking. The N–S change in structural style from thrust-sheet imbrication to detachment folding, described in Figures 7, 8, and 10, is showcased in sections C to E. The bulk of seismicity falls below the reconstructed base-salt. This implies that the base-salt is likely correctly traced in the cross sections, as the crystalline basement is expected to be more seismic than the sedimentary overburden being detached along evaporites. Moreover, the seismicity proves ongoing thick-skinned deformation beneath the Tajik basin.

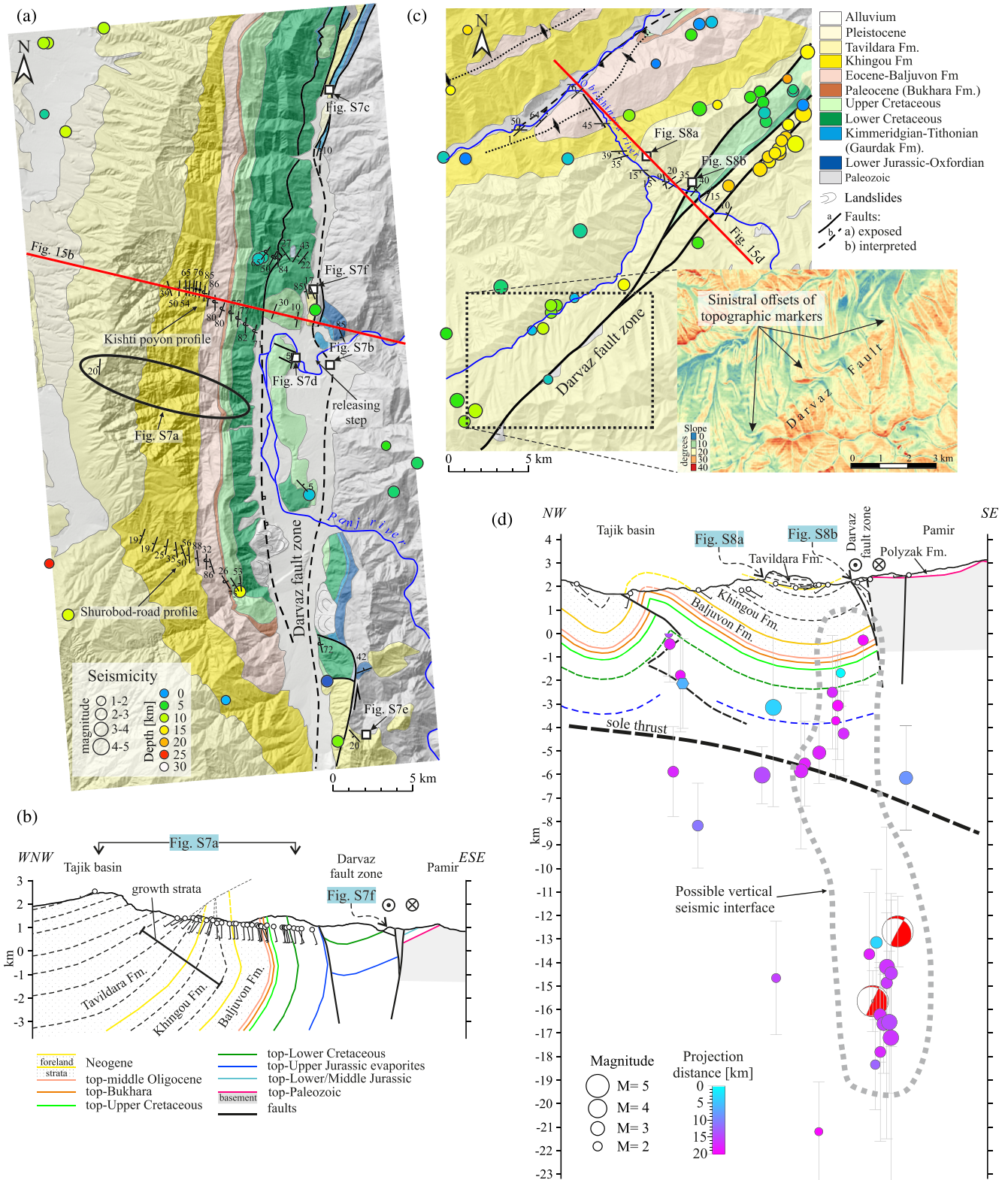


Figure 15. Eastern margin of the Tajik basin (Darvaz fault zone) in the Shurobod and “Pamir Highway” areas. Seismicity from Kufner et al. (2018); focal mechanism are cross-sectional projections. (a) Geologic map of Shurobod area. (b) Field data-based cross section along the Kishiti poyon profile, illustrating geometry of the Darvaz fault zone and the stratigraphic position of the pre-growth to growth transition. (c) Geologic map of the “Pamir Highway” area. Inset: slope map derived from a 30 × 30-m ALOS DEM showing sinistral bending of topographic markers (valleys and ridges) across the Darvaz fault zone. (d) Field data-based cross section, showing the Darvaz fault zone and stratigraphic position of the pre-growth to growth transition. Figure 2b for location of the maps and sections.

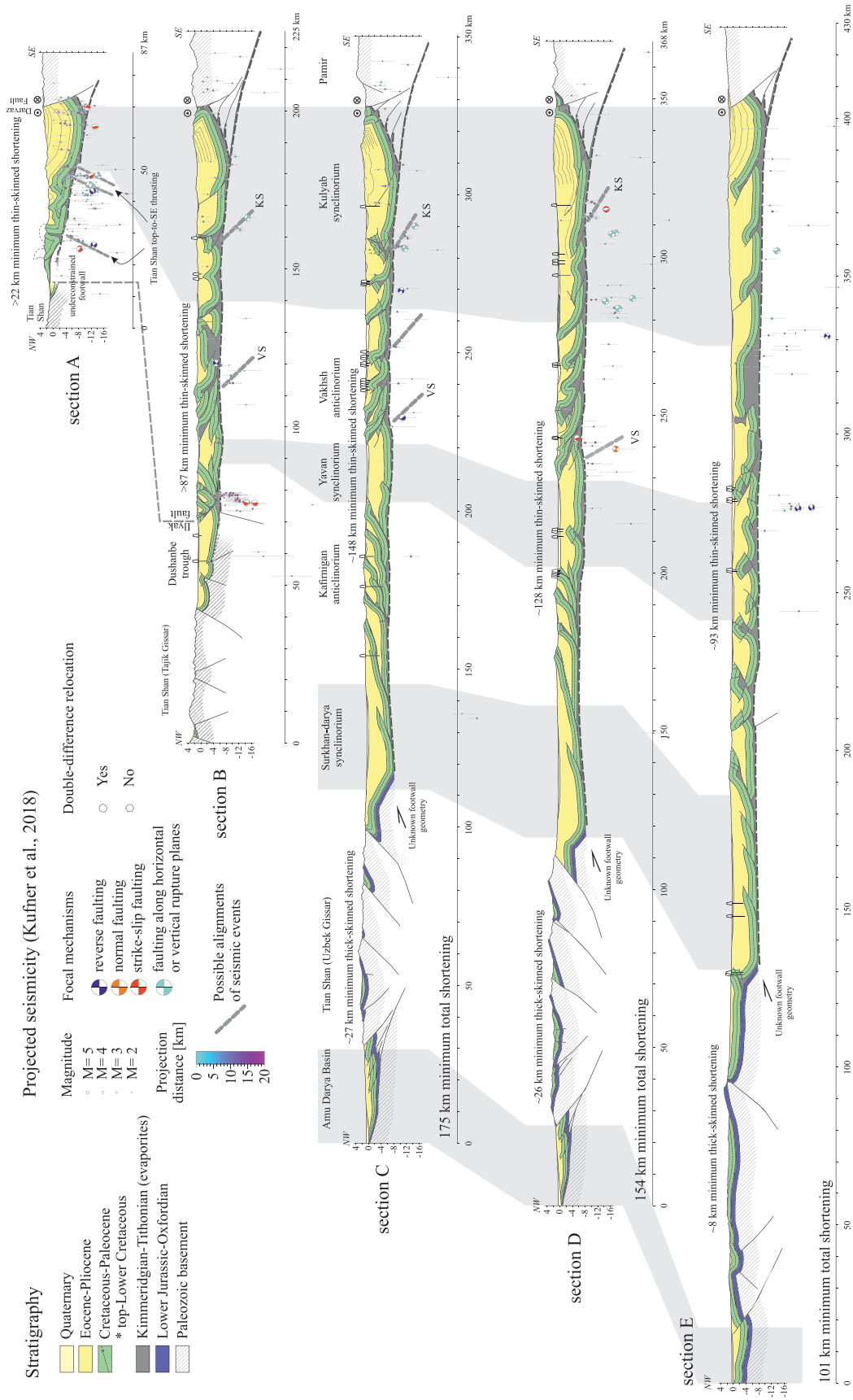


Figure 16. Cross sections through the Tajik-basin fold-and-thrust belt. The cross sections bridge all data presented in this study with gaps filled conceptually. Earthquake hypocenters and focal mechanisms (in cross-sectional projections) from Kufner et al. (2018); vertical bars give depth uncertainties.

Table 1
Shortening Estimates Along Regional Cross Sections

Cross section	Uzbek Gissar	E vergent	W vergent	Thin skinned	Total
A	n.a.	n.a.	22 ^a	22 ^a	n.a.
B	n.a.	27 ^a	60	87 ^a	n.a.
C	27	89	59	148	175
D	26	71	57	128	154
E	8	47	46	93	101

Note. Thin-skinned shortening is divided into the components accommodated by the back thrusts in the Kafirnigan anticlinorium and folds/fore-thrusts in the eastern, the internal structural zones. n.a. = not applicable or not analyzed.

^aDenotes numbers that are not representative due to erosion or termination against a lateral ramp.

The cross sections contain—despite the control by surface and subsurface data in most portions—also weakly constrained parts, where the interpretation is diagrammatic. The most important parts are as follows: (1) Footwall of the Uzbek Gissar (cross-sections C–E). The thick foreland-basin strata obscure the geometry of the eastern thrust front. Thus, it remains uncertain whether the thrust is blind or propagates into the Upper Jurassic detachment of the Tajik basin. Furthermore, this prevents the quantification of the amplitude of the thrusting of the Uzbek Gissar over the Tajik basin. (2) Surkhan-darya synclinorium. Only along cross-section E, scarce surface and borehole data constrain low-amplitude anticlines; their geometries in cross-sections C and D are conceptual. (3) Footwall of the northeastern Tajik FTB (cross-section A). Both the southeastern extent of the Cretaceous–Recent strata in the footwall of the detachment (see different models in Hamburger et al., 1992) and the position of possible NW dipping ramps in the Tian Shan base-

ment under the detachment are unconstrained. (4) Basement geometry outside areas covered by the base-salt map (Figure 4). We assume a continuation of the undulating but consistently deep basement all across the Tajik basin; this assumption conforms with the surface structural styles. (5) Geometries below the homocline stretching along the Pamir front (sections B–D). The depicted, conjectural geometry at depth is a stack of basement slices above a basal thrust that conveys shortening from the Pamir into the Tajik FTB. The homocline may represent the roof of a blind basement wedge or a triangle zone, originating from the indentation of the leading edge of the Pamir into the Upper Jurassic evaporites of the Tajik basin.

Table 1 summarizes the estimates of shortening absorbed by the Tajik FTB and Uzbek Gissar. The estimates across the Uzbek Gissar do not account for its emplacement over the basement of the Tajik basin, as this is not constrained (cross-sections C–E). The thin-skinned shortening estimate along cross-section A is not representative for the bulk shortening due to the exposed basal thrust, the unknown amount of erosion of the leading edge of northeastern Tajik FTB, and the unknown position of its footwall ramp. Cross-section B passes through the Ilyak-fault lateral ramp, and—consequently—the shortening estimate for the (S)E vergent branch of the Tajik FTB is underestimated. Therefore, the shortening estimates for cross-sections A and B describe only the internal strain absorbed by the thin-skinned structures.

6. Discussion

6.1. Thin- Versus Thick-Skinned Deformation in the Tajik Fold-and-Thrust Belt

We interpret the Tajik FTB as a thin-skinned fold-and-thrust belt detached above a basin-wide evaporitic décollement. The top-basement interpreted from seismic lines remains deep and features long-wavelength undulations. No univocal effects of basement deformation are visible in the surface data. However, seismicity shows active basement faulting (Kufner et al., 2018; McNab et al., 2019). This includes the areas covered by seismic data where the basement remains deep and relatively flat. This discrepancy between the top-basement geometry and seismicity may be due to a recent onset of basement deformation that has not yet produced a significant top-basement structural relief. The alignments of the seismic events, projected onto the cross sections, combined with the focal mechanisms, indicate reverse faults. The most prominent of them—traceable across several cross sections—are two seismic clusters: one under the Vakhsh anticlinorium (Figure 4; Figure 16, marker VS) and another under the Kulyab synclinorium (Figure 16, marker KS). Other clusters are more speculative but also highlighted in Figure 16. The seismic cluster VS underlies a base-salt high delineated on the time map (Figure 4). Regardless whether this high is a velocity pull-up or not, the basement seismicity attests to an active fault zone in this part of the Tajik-basin basement. The tight stacking of thrust sheets in the cover above this seismic cluster, including break-back geometries (Figure 10a), may be explained—in a speculative interpretation—by a disconnection of the basal detachment that triggered localized out-of-sequence thrusting in the late phase of shortening.

From seismicity, McNab et al. (2019) postulated decoupled thin-skinned, ~E-W shortening in the Tajik basin proper, and thick-skinned, ~N-S shortening in the southern, Afghan part of the Tajik basin. Clear

representations of the corresponding E-W structural trends do not appear in our data north of the Amu Darya river. An exception may be the transverse step “A” in the base-salt map (Figure 4). In addition, a few strike-slip focal-mechanism solutions with \sim N trending P axes imply subordinate N-S shortening in the Tajik basin (Figure 1b).

The base-salt map (Figure 4), indicating \leq 10-km-thick Tajik-basin deposits, and the \sim 35- to 45-km crustal thickness of the Tajik basin derived from receiver functions (Schneider et al., 2019) allow an estimate of the thickness of crystalline crust (25–35 km) under the Tajik basin. The Tajik-basin crust may serve as a proxy of the original crust connecting the Tajik basin with Tarim, now overthrust by the Pamir. Since the inclined low velocity zone representing Asian crust under the Pamir is only 10–15 km thick (Mechie et al., 2019; Schneider et al., 2013; Sippl, Schurr, Tympel, et al., 2013; Sippl, Schurr, Yuan, et al., 2013), it is probably only the lower crust that is—together with the underlying mantle lithosphere—currently rolling back beneath the Pamir (Kufner et al., 2016).

Bekker (1996) proposed a thin-skinned solution similar to ours via a combination of geologic, magnetotelluric, and gravimetric methods; it also shows a fairly flat and deep (8–12 km b.s.l.) top-basement. He explained the Kafirnigan and Vakhsh anticlinoria by stacking of thrust sheets carried along thrusts with high displacements. An alternative solution—assuming involvement of pre-Jurassic basement below the Tajik FTB to explain the intervening anticlinoria and synclinoria—was introduced by Thomas, Gapais, et al. (1994) and followed by Bourgeois et al. (1997) and Gaġala et al. (2014). Chapman et al. (2017) proposed a “double deck” structure of the Tajik FTB with an imbricate system involving sub-salt basement rocks that rise to \sim 4 and \sim 3 km b.s.l. under the Vakhsh and Kafirnigan anticlinoria, respectively. Our base-salt time map shows depths of \sim 3,000-ms TWT at these culminations. This would imply unrealistically low seismic velocities of \sim 2,600 and \sim 2,000 m/s. Besides general similarities—basement geometry and thin-skinned structures (Bekker, 1996) and salt tectonics (Thomas et al., 1996; Thomas, Gapais, et al., 1994)—our geometries are better resolved due to the numerous subsurface ties. The better defined position of the sole thrust provides a tighter constraint on the subsurface geometries of the thin-skinned structures and the amount of thin-skinned shortening. In addition, the modern seismicity outlines intra-basement faults and possible links between the thin- and thick-skinned deformation.

6.2. Thin-Skinned Structural Styles, Salt Tectonics, and Their Relation to a Late Jurassic Paleogeography

The structural styles of the Tajik FTB are best assessed in the central-southern Tajik basin where most of the thin-skinned belt is preserved due to little erosion. The seismic data demonstrate that there is a major change in structural style between the central (Figure 16; sections B–D) and southern parts of the basin (Figure 16, section E). The central part features thrust-stacks, and the southern part thrusts detachment anticlines with salt tectonics. This along-strike change in structural styles coincides with changes in the thickness and facies of the Upper Jurassic Gaurdak Fm. Its thickness along the soles of the thrust sheets in the northern Kafirnigan anticlinorium—both outcropping and pierced by boreholes—rarely exceeds 100 m (exceptional is the \sim 660-m thickness in borehole Kurgancha Severnaya 20, Figure 8a); it consists mainly of shales and mudstones with layers of gypsum (Figure S2). We observed neither direct (outcrops) nor indirect (salt springs) indicators of the presence of halite. In contrast, seismic and borehole data in the southern Tajik FTB substantiate a much thicker and more mobile evaporite section with halite dominant (Figures 7b, 8b, 10a, and 10b). Thus, the different structural styles likely depend on the original thickness and facies distribution in the Late Jurassic evaporitic basin. There is no lateral ramp between the northern and southern domains, and the anticline trends—in particular those of the Kafirnigan anticlinorium—can be traced from N to S. This indicates that—on first order—the N-S thickness and facies changes were gradational and reflect a general N-S subsidence increase in the Late Jurassic evaporitic basin.

The salt-tectonic domain in the southeastern Tajik FTB likely represents a detached and squeezed salt depositor. The observed Q-tip geometry, salt corridors, non-stratigraphic salt/sediment contacts in boreholes, and steep- to vertical, near-salt bedding attitudes are typical for squeezed diapirs. Our data suggest a Cretaceous onset of the salt tectonics, as most of the anomalous salt/sediment contacts in the boreholes are against Cretaceous strata. Yet we lack unambiguous halokinetic sequences that would prove this age assignment. In particular, we do not rule out the possibility that at least some of the salt diapirs may have originated from erosionally thinned crests of salt-cored detachment anticlines. A weakness of this

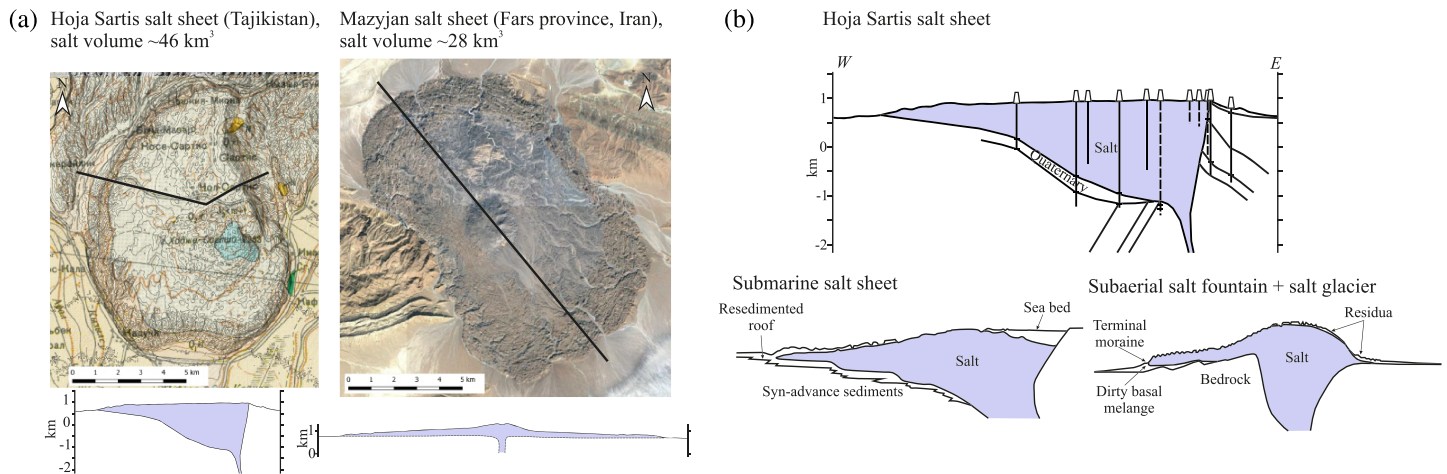


Figure 17. (a) Hoja Sartis salt sheet versus Mazyjan salt sheet (Fars province, Iran, 28°00′00.97″N, 54°54′29.46″E). Outlines of the Hoja Sartis salt sheet emphasized by dense (20 m) altitude contouring on top of Soviet-time geologic map sheets J-42-XVI, J-42-XXII. Mazyjan salt sheet image from Google Earth imagery®. (b) Hoja Sartis salt sheet versus idealized cross sections of a submarine salt sheet and a subaerial salt fountain with associated salt glaciers (simplified from Jackson & Hudec, 2017).

hypothesis is the limited erosion in the salt-tectonic domain that only exceptionally incises the top-Bukhara, which is >2,000 m higher than the stratigraphic top-salt (Figure 3).

The Late Jurassic salt depocenter of the Amu Darya basin also produced a few localized salt diapirs; similar to the Tajik basin, their time of formation is uncertain (Brunet et al., 2017). The isopach map of the Gaurdak Fm in the Amu Darya basin shows a continuation of the salt trough into the Tajik basin through the narrow corridor between the Uzbek Gissar and the Afghan platform (Figure 7c in Brunet et al., 2017). A thickness in excess of 1,200 m is indicated at the transition between these two basins. Thus, the salt domain of the southern Tajik basin is likely an extension of the evaporitic depositional system of the Amu Darya basin. However, the area of halite deposition in the southeastern Tajik basin, later generating the salt-tectonic phenomena, was most likely isolated, as the salt-tectonic geometries are absent in the western Tajik FTB, at its transition to the Amu Darya basin.

Besides the interpretation that part of the salt tectonics is Cretaceous, the seismic data (Figure 13) show univocal evidence of salt emplacement into the Neogene foreland-basin strata, that is, remnant diapirs and salt wings. This, we consider the result of salt extrusion from rejuvenated but preexisting diapirs due to foreland-basin sediment loading and shortening. The modern salt sheets represent the last phase of salt extrusion and are likely fed from squeezed Cretaceous diapirs (Hoja Sartis salt sheet, Figure 12) or from second-generation salt extrusions in the foreland-basin strata (Hoja Mumin salt sheet, Figure 13). The active subaerial salt sheets in the Tajik basin are a rare onshore example of this kind of structures, second only to the Fars salt province in Iran (e.g., Jahani et al., 2007). However, profound differences exist between these two cases. The Fars salt glaciers spill from anticlinal ridges onto mountain slopes and into valley bottoms. As a result, the salt glaciers are thin, and their lifetime depends on the interplay between erosion and salt-supply rates (Talbot, 1998). In contrast, the Tajik salt sheets extrude into a Quaternary depocenter receiving continuous clastic input. The ongoing deposition plays a role in preserving the extruded salt. Figure 17a compares the Hoja Sartis salt sheet with the Mazyjan salt sheet, the latter being one of the biggest sheets in the Fars province in terms of surface coverage. While the map dimension of the Hoja Sartis salt sheet is smaller than the Mazyjan sheet, it is at least 60% larger in terms of volume (Mazyjan salt sheet volume calculated from an ALOS DEM for the upper surface and assuming a flat base at 800 m a.s.l.). This is due to the embedding of the Hoja Sartis salt sheet in the foreland-basin strata that results in salt thickness of up to 2,000 m, much higher than in the Mazyjan salt sheet, which spills from a relay zone onto a flat valley floor. The same is true for the other salt sheets of the Tajik basin that attain thicknesses in excess of 1,000 m. The salt supply competes with the ongoing deposition, and as a result a part of the extruded salt avoids dissolution, being buried in the Quaternary strata (Figure 11). The interplay between simultaneous salt supply and deposition makes the Tajik salt sheets similar to submarine salt sheets (Figure 17b). We

conclude that multiple salt recycling arose from the main evolution phases of the Tajik basin: Cretaceous-Paleogene sagging, Neogene foreland-basin loading and shortening, and modern shortening; deposition of thick foreland-basin strata accompanied the latter two phases.

The thin-skinned anticlines of the Tajik FTB show contemporaneous onset of cooling due to shortening and erosion regardless of their distance from the Pamir (Abdulhameed et al., 2020): The oldest population of cooling ages from the Vakhsh anticlinorium spans 11.3–9.0 Ma, indicating the same age of thrusting as in the Kafirnigan anticlinorium (12.2–10.3 Ma). The more internal Kulyab synclinorium yielded one date at ~9.0 Ma (Chapman et al., 2017), again indicating an early onset of shortening. A basin-wide contemporaneous onset of shortening is not uncommon in fold-and-thrust belts on salt, in contrast with the foreland-ward deformation sequence of fold-and-thrust belts on brittle detachments (Bonini, 2007; Costa & Vendeville, 2002; Smit et al., 2003). While the rapid propagation of deformation into the basin interior along a ductile detachment is a well-recognized phenomenon (e.g., Sans et al., 1996), absorption of >50% of the shortening by ~ESE vergent thrusts in the distally situated Kafirnigan anticlinorium requires special conditions (see section 6.3).

Some anticlines in the Yavan synclinorium remained inactive after a period of erosion and subsequent burial, despite of ongoing shortening (e.g., Figure 9, section B). Analogue models indicate that sediment accumulation on top of growing anticlines retards and eventually terminates folding (Nalpas et al., 2003, 1999). The model and the Tajik-basin examples are not fully identical: The processes are about contemporaneous in the analogue models but consecutive in the Tajik basin, with successive anticline growth, erosion, and burial. Nevertheless, the increase of the sediment thickness effectively increases the preferred fold wavelength; this conceptually explains why some anticlines remained fossilized below foreland strata while others resumed their growth despite thicker overburden. The resumption of shortening in the east-central (Vakhsh anticlinorium) and easternmost Tajik FTB is the youngest event distinguished by the thermochronologic data. The out-of-sequence geometries documented in the Vakhsh anticlinorium (negative cutoff angles in Figure S3) likely are a structural record of this event.

6.3. Shortening Distribution and Its Implications

The basement of the Tajik basin was translated westward as a relatively coherent block, as suggested by its limited thick-skinned deformation. The Tajik-basin sediments also underwent paleomagnetically confirmed anticlockwise rotation of up to ~50°, although this number combines pivoting of the basement and the northward-increasing thin-skinned shortening (Thomas, Chauvin, et al., 1994). The translation and rotation were absorbed by the thick-skinned thrusting in the Uzbek Gissar and the dextral transpression in the Tajik Gissar. In the latter, Käbner et al. (2016) documented an array of Cenozoic longitudinal faults outlined by synclines filled with Triassic-Neogene strata. These faults permit a slip transfer from the advancing Pamir into the horsetail thrusts of the Uzbek Gissar. Thus, the thick-skinned shortening in the Uzbek Gissar—estimated at ~27 km near its junction with the Tajik Gissar (Figure 16, section C; Table 1)—should equal the composite amount of the strike-slip offset along the longitudinal faults in the Tajik Gissar. The thick-skinned shortening in the Uzbek Gissar and the westward displacement of the Tajik-basin basement require a deep detachment. This detachment must be kinematically linked to the crustal convergence, crustal thickening, and lateral flow deformation field in the Pamir (e.g., Kufner et al., 2018; Schneider et al., 2019; Schurr et al., 2014; Stübner et al., 2013).

Our thin-skinned shortening estimates summarized in Table 1 fall in between the most (Chapman et al., 2017) and least (Bourgeois et al., 1997) conservative calculations presented so far. We stress the importance of borehole data to pinpoint the minimum distances of tectonic duplications, in particular in the Kafirnigan anticlinorium that accounts for >50% of the total shortening. The only structural interpretation published so far that made an extensive use of borehole data is that of Bekker (1996). As a result, his structural scheme and shortening estimates are similar to ours. For example, Bekker's (1996) cross-section B estimated ~154 km of thin-skinned shortening as compared to ~148 km from our nearby located cross-section C (Figure 16). Conversely, missing or incomplete borehole data led to the vague estimations of the amounts of shortening. For example, the Kurgancha 21 well terminates in the Cretaceous strata of the Babatag thrust sheet in Figure 3 of Chapman et al. (2017). According to our well-top database, confirmed by a legacy Soviet-time report (Kukushkin, unpublished report, 1976) and cross-section B in Bekker (1996), it penetrated the Babatag thrust-sheet sole thrust and entered a structurally lower

thrust sheet. Consequently, the amount of displacement of the Babatag thrust sheet is approximately twice as in Chapman et al. (2017).

Kinematic consistency requires that the thin-skinned shortening of the Tajik FTB is compensated along the margins of the Tajik basin by thick-skinned thrusting. Given the regional tectonics, the ultimate source of the tectonic shortening is the zone of crustal convergence in the Pamir. A challenge to this rule is the apparently vertical Darvaz fault zone with the earthquake hypocenters forming a subvertical alignment reaching down to ~20 km b.s.l. in the northeastern Tajik basin (Figure 15d). This is at odds with the thin-skinned shortening of the Tajik FTB that cannot be conveyed across a vertical fault interface. One may consider the pattern of seismicity a coincidental superposition of two sources of seismicity: a shallow one linked to the Darvaz fault zone proper and a deep one related to a local source in the basement below the thin-skinned sole thrust. Alternatively, if the seismic events in Figure 15d represent a single fault interface, it must be a young feature, largely post-dating the thin-skinned thrusting in the Tajik FTB (cf. Kufner et al., 2018).

A central question of the large-scale kinematics of the Tajik FTB is the role played by the Uzbek Gissar. Is it a buttress to the thin-skinned system or a zone of crustal convergence contributing to the total shortening budget of the Tajik FTB? The former scenario dominates the previous interpretations (Bekker, 1996; Bourgeois et al., 1997; Burtman, 2000; Thomas et al., 1996; Thomas, Gapais, et al., 1994); Chapman et al. (2017) introduced the latter. Thus, two end-member kinematic solutions may be considered for the southern Tajik FTB (Figure 18a). Model 1 assumes that the Uzbek Gissar is a semi-passive buttress and the bulk of the shortening is conveyed to the sedimentary fill of the Tajik basin along the frontal ramp of the Pamir. According to this solution, the Kafirnigan anticlinorium is a stack of back thrusts, and the Yavan synclinorium is a zone of vergence change. Model 2 postulates underthrusting of the Tajik-basin basement below the Uzbek Gissar by the amount equal to the shortening absorbed by the ~ESE vergent Kafirnigan anticlinorium. In Model 2, the Tajik FTB consists of two separate, oppositely vergent fold-and-thrust belts, colliding along the Yavan synclinorium. The latter is the common foreland syncline and—on first order—remains in its original position with respect to the Tajik-basin basement (Figure 3b in Chapman et al., 2017).

In our opinion, Model 2 may work only for low displacements. Chapman et al. (2017) calculated 35–45 km of shortening for the Kafirnigan anticlinorium that was conveyed from the Uzbek Gissar. According to our estimate, the shortening absorbed by the Kafirnigan anticlinorium reaches ~89 km (cross-section C, Table 1). If it was conveyed ESE from a zone of crustal stacking below the Uzbek Gissar, it would have its expression in an increased Moho depth that is not evident (thick, dotted line in Figure 18a; Robert et al., 2017; Schneider et al., 2019). Moreover, lateral accommodation of such a big, yet localized shortening is another problem, as no transfer faults with sufficiently high strike-slip displacements can be identified on either end of the Uzbek Gissar. For example, if the Tajik-basin crust is underplated below the Uzbek Gissar by ~89 km, it requires a crustal-scale dextral transfer fault zone along the southern edge of the Tajik Gissar. The Ilyak fault zone is an obvious candidate. However, such a high displacement at the basement level is difficult to justify, given the fact that the Ilyak fault has no expression—neither geologic nor seismologic—west of the Kafirnigan anticlinorium. Moreover, this high displacement shall be preserved east and north of the Ilyak fault. One possibility is thrusting of the Tian Shan over the northeastern Tajik basin by an amount similar to that of the Uzbek Gissar (variant A in the map of Model 2, Figure 18a). Another is the continuation of the Ilyak fault below the Tajik FTB into the Pamir (variant B in the map of Model 2). In contrast, Model 1 requires only limited displacement along the northern edge of the Tajik basin. This may be accommodated by the Ilyak fault and along the northern edge of the Dushanbe trough in the Tajik Gissar. Limited shortening is also easier to resolve in the northeastern Tajik basin by a limited top-to-SE thrusting of the Tian Shan, as conceptually depicted in cross-section A of Figure 16. Therefore, we consider the buttress model (Model 1, Figure 18a), following Bekker (1996), Thomas, Gapais, et al. (1994), Thomas et al. (1996), Bourgeois et al. (1997), and Burtman (2000), as more appropriate.

Adoption of Model 1 raises the question on the mechanical conditions behind the formation of the ~E vergent imbricate belt of the Kafirnigan anticlinorium. This challenge is amplified by the fact that the Kafirnigan anticlinorium consumes as much as ~60%, 55%, and 50% of the total thin-skinned shortening along cross-sections C, D, and E, respectively. The classic and solitary example showing a similar scenario is the offshore Cascadia accretionary wedge (Adam et al., 2004; Booth-Rea et al., 2008;

Gutscher et al., 2001). The western Tajik FTB would be the second—the only onshore example—of a dominantly hinterland-vergent fold-and-thrust belt. Although back thrusts are common in nearly every fold-and-thrust belt, no universal explanation exists for the consistent hinterland vergence. Potential factors proposed to account for this phenomenon are extraordinary reduction of the basal friction, mechanical stratification of the basal ductile layer, change in the shortening rate, and/or the dip of the basal detachment (Bonini, 2007; Dickinson & Seely, 1979; Gutscher et al., 2001; MacKay, 1995; MacKay et al., 1992). None of the above can be readily applied to the Tajik FTB case. Instead, we speculate that the Uzbek Gissar foreland buttress might have played a role. Abdulhameed et al. (2020) showed that the thick-skinned Uzbek Gissar started to grow coevally with the thin-skinned Kafirnigan anticlinorium. Hence, the buttress was created early in the process of the Tajik FTB buildup. Despite of the small amount of shortening transferred to the Tajik basin from the Uzbek Gissar in Model 1, it might have been sufficient to disable preferred foreland vergence. Alternatively, the hinterland-vergent thrusts might have originated at the leading edge of a short-lived system in front of the Uzbek Gissar, being later amplified and incorporated into the Tajik FTB when a wave of deformation conveyed from the Pamir reached the western part of the Tajik basin. In the latter scenario, a certain, although limited amount of thrusting of the Uzbek Gissar over the Tajik basin is required, implying a sort of hybrid solution between Models 1 and 2 (Figure 18a).

To highlight the regional implications of our shortening estimates, we performed a first-order map-view restoration (Figure 18b) and compiled a crustal-scale cross section (Figure 18c). The map-view restoration combines our shortening estimates and ages with those from the northern Pamir front (Coutand et al., 2002; Li et al., 2019); the crustal-scale cross section integrates our cross-section C (Figure 16) with geophysical constraints on deep crustal geometries: the Moho geometry from Schneider et al. (2019) and intermediate-depth seismicity from Sippl, Schurr, Yuan, et al. (2013), the latter projected within a 10-km swath. As indicated in Table 1, values yielded by cross-sections C, D, and E may be considered representative for the total shortening across the Tajik FTB. We drew curved convergence paths, corresponding to the rotations of the thin-skinned structures determined by the paleomagnetic studies in the eastern Tajik basin (section 2; Thomas, Chauvin, et al., 1994). The present ~N strike of the western edge of the Pamir restores to a ~NE strike (Figure 18b). This geometry corresponds to a pre-~12-Ma paleogeography, given the dating by Abdulhameed et al. (2020). According to Coutand et al. (2002) and Li et al. (2019), deformation along the northern sector of the Pamir orocline may have started at ~20–25 Ma. Low shortening values provided by these authors indicate that the northern deformation front was already close to its present-day position at ~12 Ma. Integration of these constraints points to the existence of a Pamir orocline before the thin-skinned shortening in the Tajik FTB commenced. Although the existence of a late Paleogene-Neogene orocline is a cornerstone in all tectonic scenarios of the Pamir, its outline remains unconstrained; if the shortening values and timing integrated in Figure 16 are correct, then these approximate the orocline's transient shape. It is possible that the shortening estimates from the Main Pamir thrust system are significantly underestimated due to the restoration of only parts of the fold-and-thrust belt (Coutand et al., 2002) and an unconstrained (Coutand et al., 2002) and poorly constrained (Li et al., 2019) extent of the foreland-basin series in the footwall of the Main Pamir thrust.

A similar issue of a “missing” shortening is evident in cross-section A where restoration yielded only ~22 km (Table 1). Buttressing by the Tian Shan narrows the thin-skinned system to <50 km in the northeastern Tajik basin. As this does not result in tighter stacking of the thin-skinned structures (Figure 16; cf. cross-section A to B–E), the shortening values are low. To mitigate the shortening deficit, Hamburger et al. (1992) considered large-scale thrusting of the northeastern Tajik FTB over semi-autochthonous Cretaceous-Cenozoic strata of the Tian Shan in the footwall of the detachment, resulting in a complete tectonic duplication and >60 km of shortening. This solution is supported by drastic thickness contrasts of the Cretaceous-Paleocene formations across the Tajik FTB frontal thrust. Another possibility was invoked by Pavlis et al. (1997), who proposed syn-tectonic erosion of the deformation front of the Tajik FTB by the Surkhob longitudinal trunk stream, channeled between the Tian Shan and the advancing thin-skinned belt (Figure 14); only the internal portions of the thin-skinned system are preserved in the northeastern Tajik basin according to this scenario, most of the fold-and-thrust belt being pushed up against the slope of the Tian Shan and eroded. These possibilities are not mutually exclusive, and both may contribute to the missing shortening with respect to the central-southern part of the Tajik FTB.

Figure 18c illustrates the constraints imposed by the Tajik FTB foreland shortening on the geometry of the Tajik-basin lithosphere (Pamir slab) beneath the Pamir. Sippl, Schurr, Tympel, et al. (2013) interpreted the subvertical cluster of seismicity between ~100- and 200-km depth as representing eclogitized Asian (Tajik) lower crust, overlain between 60 and 100 km by subducted middle crust. Thus, the seismicity cluster and the subducted middle crust approximate the downdip extension of the detachment(s) of the Tajik FTB. If so, this geometry defines the curved upper interface of the downgoing Tajik-basin crust; this geometry is mimicked by the Tajik Moho down to ~90 km. The Tajik mantle lithosphere was tomographically imaged to go deeper—beyond 300 km (Kufner et al., 2016)—than the seismicity. If the Tajik FTB shortening estimates are considered a proxy to the amount of convergence, then the ≥ 148 km of shortening yielded by cross-section C, or ≥ 175 km if the shortening of the Uzbek Gissar is also transferred to the Pamir convergence zone, this is not enough to account for the underthrusting the Tajik lithosphere as delineated by the seismicity and tomography; this is consistent with the conclusion of Chapman et al. (2017). A possible solution to this discrepancy would be accretion of substantial amounts of Tajik upper and middle crust in the North Pamir, while the Tajik mantle lithosphere and possibly lower crust rolls back (Figure 18c). Testing his hypothesis needs quantification of post-~12 Ma shortening in the North Pamir, if it is correct that rollback of the slab below the Pamir started at ~12 Ma (Kufner et al., 2016). The deep-reaching seismic zone would in this scenario constitute an incomplete Tajik lithosphere, deprived of its middle and upper crustal layer, the middle crust partly subducted to 80–100 km, and—together with the upper crust—accreted to the hanging wall and forming the North Pamir and the Tajik FTB. Chapman et al. (2017) proposed that also Central Pamir lithosphere must be involved into the rollback process, however, using much smaller shortening estimates (65–70 km) across the Tajik FTB as derived in this study.

7. Conclusions

The subsurface of the Tajik basin has remained poorly resolved due to limited availability of borehole and seismic data. Herein, we presented a basin-scale structural model based on integrated surface, borehole, seismic, and seismologic data. The wide use of subsurface constraints reduces the margin of uncertainty concerning structural styles and deep geometries. Our main findings are as follows:

1. The Tajik fold-and-thrust belt (Tajik FTB) is a thin-skinned belt developed above a basin-wide evaporitic detachment. Structural effects of basement deformation are inconclusive in the subsurface data. The occurrence of seismicity clusters, in particular in the eastern and northeastern Tajik basin, indicates active deformation in the sub-detachment basement.
2. The thick-skinned structures of the southwestern Tian Shan foreland buttress—the Uzbek and Tajik Gissar—confine the available space for the development of the Tajik FTB. The change in width of the Tajik FTB is accommodated by a major lateral ramp, the Ilyak fault zone, which parallels the northern edge of the Tajik basin.
3. The amount of thin-skinned shortening recorded in the Tajik FTB changes along strike. In the weakly eroded central-southern Tajik FTB, the shortening increases from ~93 km in the south to ~148 km in the north. This shortening increase complies with the westward-decreasing anticlockwise material rotation, documented paleomagnetically in the northern Tajik FTB. In contrast, the northeastern Tajik FTB yielded a low shortening estimate of ~22 km. Underconstrained footwall geometries and syn-tectonic erosion of the orogenic front veil an unknown portion of the orogenic shortening. The narrow northeastern Tajik FTB may represent only the remnant, most internal zone of a once much more extensive thin-skinned belt that was forced to emerge and was syn-tectonically eroded along the buttress created by the Tian Shan.
4. The internal structure of the Tajik FTB is laterally diversified by the rheology of the basal detachment in Upper Jurassic evaporites and the distribution of the syn-orogenic sediments. In the south, it includes upright detachment anticlines and bivergent thrust sheets pointing at unconfined detachment folding under a symmetric stress field with the main compression axis parallel to the basal detachment. The western Tajik FTB is a spectacular, hinterland-vergent imbricate stack.
5. Salt tectonics operates in the southeastern part of the Tajik basin. Subaerial salt sheets and salt fountains are one of few of their kind worldwide, subordinate only to the Zagros fold belt. They originate from pre-existing (Cretaceous) salt diapirs, squeezed and reworked in the course of late Neogene tectonic

shortening. The southern Tajik basin represents the second depocenter of the larger Amu Darya-Tajik salt province after the one described earlier in the Amu Darya basin.

6. Low-temperature thermochronology and observations of growth strata indicate a basin-wide onset of folding and thrusting in a short interval, ~12–9 Ma. This supports a non-Coulomb behavior of the Tajik FTB in accordance with its evaporitic sole.
7. To reconcile the deficit between the shortening in the Tajik FTB and the thick-skinned foreland buttress of the Uzbek Gissar and the rollback of the Tajik lithosphere (the Pamir slab) as delineated by seismicity and tomography, shortening and accretion of substantial amounts of Tajik upper and middle crust must have occurred in the North Pamir.

Acknowledgments

Additional data are given in the supporting information and can be downloaded online (from <https://opara.zih.tu-dresden.de/xmlui/handle/123456789/1682?locale-attribute=en>). Deutsche Forschungsgemeinschaft (DFG) bundle TIPAGE (PAK 443), project CLIENT II - CaTeNA of the German Federal Ministry of Education and Research (Support Code 03G0809), and a research grant from TOTAL to TU Bergakademie Freiberg funded this work. S. A. received scholarships from Damascus University and the State of Saxony. M. Franz, B. Sperner, and A. Szulc contributed to fieldwork. TU Bergakademie Freiberg acknowledge an academic license of the Petroleum Experts Limited Move software. Jonas Kley and an anonymous referee provided stimulating reviews. Work in Tajikistan and Uzbekistan would have been impossible without the support of the Tajik and Uzbek Academy of Sciences. This paper is part of the doctoral thesis of Lukasz Gągała at TU Bergakademie Freiberg.

References

- Abdulhameed, S., Ratschbacher, L., Jonckheere, R., Gągała, L., Enkelmann, E., Kars, M., et al. (2020). Tajik Basin and southwestern Tian Shan, northwestern India-Asia collision zone: 2. Timing of basin inversion, Tian Shan mountain building, and relation to Pamir-Plateau collapse and deep India-Asia Indentation. *Tectonics*, 39. <https://doi.org/10.1029/2019TC005873>
- Adam, J., Klaeschen, D., Kukowski, N., & Flueh, E. (2004). Upward delamination of Cascadia Basin sediment infill with landward frontal accretion thrusting caused by rapid glacial age material flux. *Tectonics*, 23(3), TC3009. <https://doi.org/10.1029/2002TC001475>
- Bekker, Y. A. (1996). Tectonics of the Afghan-Tajik basin. *Geotektonika*, 1, 76–82. (in Russian)
- Bonini, M. (2007). Deformation patterns and structural vergence in brittle-ductile thrust wedges: An additional analogue modelling perspective. *Journal of Structural Geology*, 29(1), 141–158. <https://doi.org/10.1016/j.jsg.2006.06.012>
- Booth-Rea, G., Klaeschen, D., Grevemeyer, I., & Reston, T. (2008). Heterogeneous deformation in the Cascadia convergent margin and its relation to thermal gradient (Washington, NW USA). *Tectonics*, 27, TC4005. <https://doi.org/10.1029/2007TC002209>
- Bosov, V. D. (1972). *Tertiary continental deposits of Tajikistan*. Dushanbe, USSR: Donish. (in Russian)
- Bourgeois, O., Cobbold, P. R., Rouby, D., & Thomas, J.-C. (1997). Least squares restoration of Tertiary thrust sheets in map view, Tajik depression, central Asia. *Journal of Geophysical Research*, 102, 27,553–27,573.
- Brookfield, M. E., & Hashmat, A. (2001). The geology and petroleum potential of the North Afghan platform and adjacent areas (northern Afghanistan, with parts of southern Turkmenistan, Uzbekistan and Tajikistan). *Earth-Science Reviews*, 55, 41–71.
- Brunet, M.-F., Ershov, A. V., Korotaev, M. V., Melikhov, V. N., Barrier, E., Mordvintsev, D. O., & Sidorova, I. P. (2017). Late Palaeozoic and Mesozoic evolution of the Amu Darya Basin (Turkmenistan, Uzbekistan). In M.-F. Brunet, T. McCann, & E. R. Sobel (Eds.), *Geological evolution of Central Asian basins and the western Tien Shan range* (Vol. 427, pp. 89–144). London: Geological Society, London, Special Publications. <https://doi.org/10.1144/SP427.18>
- Burtman, V. S. (2000). Cenozoic crustal shortening between the Pamir and Tien Shan and a reconstruction of the Pamir-Tien Shan transition zone for the Cretaceous and Paleogene. *Tectonophysics*, 319, 69–92.
- Burtman, V. S., & Molnar, P. (1993). Geological and geophysical evidence for deep subduction of continental crust beneath the Pamir. *Special Paper Geological Society of America*, 281, 1–76.
- Butler, R. W. H., Bond, C. E., Cooper, M. A., & Watkins, H. (2019). Fold-thrust structures—Where have all the buckles gone? In C. E. Bond, & H. D. Lebit (Eds.), *Folding and fracturing of rocks: 50 years of research since the seminal text book of J. G. Ramsay*, (Vol. 487, pp. 21–44). London: Geological Society, London, Special Publications. <https://doi.org/10.1144/SP487.7>
- Carrapa, B., DeCelles, P. G., Wang, X., Clementz, M. T., Mancin, N., Stoica, M., et al. (2015). Tectono-climatic implications of Eocene Paratethys regression in the Tajik basin of central Asia. *Earth and Planetary Science Letters*, 424, 168–178. <https://doi.org/10.1016/j.epsl.2015.05.034>
- Chapman, J. B., Carrapa, B., Ballato, P., DeCelles, P. G., Worthington, J., Oimahmadov, I., et al. (2017). Intracontinental subduction beneath the Pamir Mountains: Constraints from thermokinematic modeling of shortening in the Tajik fold-and-thrust belt. *Geological Society American Bulletin*, 129, 1450–1471. <https://doi.org/10.1130/B31730.1>
- Chapman, J. B., Carrapa, B., DeCelles, P. G., Worthington, J., Mancin, N., Cobiainchi, M., et al. (2019). The Tajik basin: A composite record of sedimentary basin evolution in response to tectonics in the Pamir. *Basin Research*. <https://doi.org/10.1111/bre.12381>
- Costa, E., & Vendeville, B. C. (2002). Experimental insights on the geometry and kinematics of fold-and-thrust belts above weak, viscous evaporitic decollement. *Journal of Structural Geology*, 24, 1729–1739.
- Coutand, I., Strecker, M. R., Arrowsmith, J. R., Hilley, G., Thiede, R. C., Korjenkov, A., & Omuraliev, M. (2002). Late Cenozoic tectonic development of the intramontane Alai Valley, (Pamir-Tien Shan region, central Asia): An example of intracontinental deformation due to the Indo-Eurasia collision. *Tectonics*, 21(6), 1053. <https://doi.org/10.1029/2002TC001358>
- Dahlstrom, C. D. A. (1969). Balanced cross sections. *Canadian Journal of Earth Sciences*, 6, 743–757.
- Dedow, R., Franz, M., Szulc, A., Schneider, J. W., Brückner, J., Ratschbacher, L., et al. (2020). Tajik Basin and southwestern Tian Shan, northwestern India-Asia collision zone: 3. Preorogenic to syn orogenic retro-foreland basin evolution in the eastern Tajik depression and linkage to the Pamir hinterland. *Tectonics*, 39. <https://doi.org/10.1029/2019TC005874>
- Dickinson, W. R., & Seely, D. R. (1979). Structure and stratigraphy of forearc regions. *AAPG Bulletin*, 63, 2–31.
- Doeblich, J. L., & Wahl, R. R. Compilers (2006). *Geological and mineral resource map of Afghanistan; version 2*. Reston, VA: U.S. Geol. Surv. Open File Rep. 2006–1038.
- Forsten, A., & Sharapov, S. (2000). Fossil equids (Mammalia, Equidae) from the Neogene and Pleistocene of Tadzhikistan. *Geodiversitas*, 22, 293–314.
- Gągała, L. (2014). *Structural geometry and kinematics of the Tajik depression, Central Asia: Neogene basin inversion in front of the Pamir salient (doctoral dissertation)*. <http://swbplus.bsz-bw.de/bsz420285989inh.htm>. Germany: Technische Universität Bergakademie Freiberg.
- Gągała, L., Käfner, A., Abdulhameed, S., Szulc, A., Ratschbacher, L., Ringenbach, J.-C., et al. (2014). Structure and exhumation of the Tajik Depression (western foreland of the Pamir): Towards an integrated kinematic model. Paper presented at 14th International Conference on Thermochronology, Chamonix, France.
- GRI (1961–1984). *Geological maps of the Soviet Union 1:200,000, Alai-Gissar, Pamir and South Tajikistan Series*. Nedra, Moscow: Russ. Geol. Res. Inst. (in Russian)

- Gutscher, M.-A., Klaeschen, D., Flueh, E., & Malavielle, J. (2001). Non-Coulomb wedges, wrong-way thrusting, and natural hazards in Cascadia. *Geology*, *29*, 379–382.
- Hamburger, M. W., Sarewitz, D. R., Pavlis, T. L., & Popandopulo, G. A. (1992). Structural and seismic evidence for intracontinental subduction in the Peter the First Range, central Asia. *Geological Society of America Bulletin*, *104*, 397–408.
- Ischuk, A., Bendick, R., Rybin, A., Molnar, P., Khan, S. F., Kuzikov, S., et al. (2013). Kinematics of the Pamir and Hindu Kush regions from GPS geodesy. *Journal of Geophysical Research, Solid Earth*, *118*, 2408–2416. <https://doi.org/10.1002/jgrb.50185>
- Jackson, M. P. A., & Hudec, M. R. (2017). *Salt tectonics. Principles and practice*. Cambridge, UK: Cambridge University Press. <https://doi.org/10.1017/9781139003988>
- Jahani, S., Callot, J.-P., Frizon de Lamotte, D., Letouzey, J., & Leturmy, P. (2007). The salt diapirs of the eastern Fars Province (Zagros, Iran): A brief outline of their past and present. In O. Lacombe, J. Lavé, F. M. Roure, & J. Vergès (Eds.), *Thrust belts and foreland basins: From fold kinematics to hydrocarbon systems. Frontiers in Earth Sciences*, (pp. 289–308). Berlin, Heidelberg: Springer.
- Jepson, G., Glorie, S., Konopelko, D., Gillespie, J., Danišik, M., Evans, N. J., et al. (2018). Thermochronological insights into the structural contact between the Tian Shan and Pamirs, Tajikistan. *Terra Nova*, *30*, 95–104. <https://doi.org/10.1111/ter.12313>
- Käbner, A., Ratschbacher, L., Jonckheere, R., Enkelmann, E., Khan, K., Sonntag, B.-L., et al. (2016). Cenozoic intracontinental deformation and exhumation at the northwestern tip of the India-Asia collision—Southwestern Tian Shan, Tajikistan, and Kyrgyzstan. *Tectonics*, *35*(9), 2171–2194. <https://doi.org/10.1002/2015TC003897>
- Klocke, M., Voigt, T., Kley, J., Pfeifer, S., Rocktäschel, T., Keil, S., Gaupp, R. (2017). Cenozoic evolution of the Pamir and Tien Shan mountains reflected in syntectonic deposits of the Tajik Basin. In M.-F. Brunet, T. McCann, E. R. Sobel (Eds.), *Geological evolution of Central Asian basins and the western Tien Shan range* (Vol. 427, pp. 523–564). London: Geological Society, London, Special Publications. <https://doi.org/10.1144/SP427.7>
- Kuchai, V. K., & Trifonov, V. G. (1977). Young left-lateral strike slip along the zone of the Darvaz-Karakul fault. *Geotektonika*, *3*, 91–105. (in Russian)
- Kufner, S.-K., Schurr, B., Ratschbacher, L., Abdulhameed, S., Murodkulov, S., & Metzger, S. (2018). Seismotectonics of the Tajik basin and surrounding mountain ranges. *Tectonics*, *37*(8), 2404–2424. <https://doi.org/10.1029/2017TC004812>
- Kufner, S.-K., Schurr, B., Sippl, C., Yuan, X., Ratschbacher, L., Ischuk, A., et al. (2016). Deep India meets deep Asia: Lithospheric indentation, delamination and break-off under Pamir and Hindu Kush (central Asia). *Earth and Planetary Science Letters*, *435*, 171–184. <https://doi.org/10.1016/j.epsl.2015.11.046>
- Leith, W., & Alvarez, W. (1985). Structure of the Vakhsh fold-and-thrust belt, Tajik SSR: Geologic mapping on a Landsat image base. *Geological Society of America Bulletin*, *96*, 875–885.
- Li, T., Chen, Z., Chen, J., Thompson Jobe, J. A., Burbank, D. W., Li, Z., et al. (2019). Along-strike and downipid segmentation of the Pamir frontal thrust and its association with the 1985 Mw 6.9 Wuqia earthquake. *Journal of Geophysical Research-Solid Earth*, *124*, 9890–9919. <https://doi.org/10.1029/2019JB017319>
- MacKay, M. E. (1995). Structural variations and landward vergence at the toe of the Oregon accretionary prism. *Tectonics*, *14*, 1309–1320.
- MacKay, M. E., Moore, G. F., Cochrane, G. R., Moore, J. C., & Kulm, L. D. (1992). Landward vergence and oblique structural trends in the Oregon margin accretionary prism: Implications and effect on fluid flow. *Earth and Planetary Science Letters*, *109*(3-4), 477–491. [https://doi.org/10.1016/0012-821X\(92\)90108-8](https://doi.org/10.1016/0012-821X(92)90108-8)
- McNab, F., Sloan, R. A., & Walker, R. T. (2019). Simultaneous orthogonal shortening in the Afghan-Tajik Depression. *Geology*, *47*(9), 862–866. <https://doi.org/10.1130/G46090.1>
- Mechie, J., Schurr, B., Yuan, X., Schneider, F., Sippl, C., Minaev, V., et al. (2019). Observations of guided waves from the Pamir seismic zone provide additional evidence for the existence of subducted continental lower crust. *Tectonophysics*, *762*, 1–16. <https://doi.org/10.1016/j.tecto.2019.04.007>
- Nalpas, T., Gapais, D., Verges, J., Barrier, L., Gestain, V., Leroux, G., et al. (2003). Effects of rate and nature of syn-kinematic sedimentation on the growth of compressive structures constrained by analogue models and field examples. In T. McCann, & A. Saintot (Eds.), *Tracing tectonic deformation using the sedimentary record*, (Vol. 208, pp. 307–319). London, UK: Geological Society, London, Special Publications. <https://doi.org/10.1144/GSL.SP.2003.208.01.05>
- Nalpas, T., Gyorfi, I., Guillocheau, F., Lafont, F., & Homewood, P. (1999). Influence de la charge sédimentaire sur le développement d'anticlinaux synsédimentaires. Modélisation analogique et exemple de terrain (bordure sud du bassin de Jaca). *Bulletin de la Société Géologique de France*, *170*(5), 733–740.
- Nikolaev, V. G. (2002). Afghan-Tajik depression: Architecture of sedimentary cover and evolution. *Russian Journal of Earth Sciences*, *4*(6), 399–421.
- Nikonov, A. A. (1975). An analysis of tectonic movements along the Hindu Kush-Darvaz-Karakul fault zone in late Pliocene and Quaternary time. *Izvestiya Akademii Nauk USSR, Earth Physics*, *12*, 71–76. (in Russian)
- Pavlis, T. L., Hamburger, M. W., & Pavlis, G. L. (1997). Erosional processes as a control on the structural evolution of an actively deforming fold and thrust belt: An example from the Pamir-Tien Shan region, central Asia. *Tectonics*, *16*, 810–822.
- Perry, M., Kakar, N., Ischuk, A., Metzger, S., Bendick, R., Molnar, P., & Mohadjer, S. (2019). Little geodetic evidence for localized Indian subduction in the Pamir-Hindu Kush of Central Asia. *Geophysical Research Letters*, *46*, 109–118. <https://doi.org/10.1029/2018GL080065>
- Pozzi, J.-P., & Feinberg, H. (1991). Paleomagnetism in the Tajikistan: Continental shortening of European margin in the Pamirs during Indian Eurasian collision. *Earth and Planetary Science Letters*, *103*, 365–378.
- Robert, A. M. M., Fernandez, M., Jimenez-Munt, I., & Verges, J. (2017). Lithospheric structure in Central Eurasia derived from elevation, geoid anomaly and thermal analysis. In M.-F. Brunet, T. McCann, E. R. Sobel (Eds.), *Geological evolution of Central Asian basins and the western Tien Shan range*. London, UK: Geological Society, London, Special Publications (Vol. 427, pp. 271–293). <https://doi.org/10.1144/SP427.10>
- Sans, M., Munoz, J. A., & Verges, J. (1996). Triangle zone and thrust wedge geometries related to evaporitic horizons (southern Pyrenees). *Bulletin of Canadian Petroleum Geology*, *44*, 375–384.
- Schneider, F. M., Yuan, X., Schurr, B., Mechie, J., Sippl, C., Haberland, C., et al. (2013). Seismic imaging of subducting continental lower crust beneath the Pamir. *Earth and Planetary Science Letters*, *375*, 101–112. <https://doi.org/10.1016/j.epsl.2013.05.015>
- Schneider, F. M., Yuan, X., Schurr, B., Mechie, J., Sippl, C., Kufner, S.-K., et al. (2019). The crust in the Pamir: Insights from receiver functions. *Journal of Geophysical Research: Solid Earth*, *124*(8), 9313–9331. <https://doi.org/10.1029/2019JB017765>
- Schurr, B., Ratschbacher, L., Sippl, C., Gloaguen, R., Yuan, X., & Mechie, J. (2014). Seismotectonics of the Pamir. *Tectonics*, *33*(8), 1501–1518. <https://doi.org/10.1002/2014TC003576>
- Schwab, G., Katzung, G., Ludwig, A. O., & Lütznier, H. (1980). Neogene Molasse-Sedimentation in der Tadschikischen Depression (tadschikische SSR). *Zeitschrift der Angewandten Geologie*, *26*, 225–238. (in German)

- Sherba, I. G. (1990). The reflection of the phases of Alpine tectonogenesis in the Mesozoic-Cenozoic rocks of the southern Tien Shan region. *Geotectonics*, *24*, 125–134.
- Sippl, C., Ratschbacher, L., Schurr, B., Krumbiegel, C., Rui, H., Pingren, L., & Abdybachev, U. (2014). The 2008 Nura earthquake sequence at the Pamir-Tian Shan collision zone, southern Kyrgyzstan. *Tectonics*, *33*(12), 2382–2399. <https://doi.org/10.1002/2014TC003705>
- Sippl, C., Schurr, B., Tympel, J., Angiboust, S., Mechie, J., Yuan, X., et al. (2013). Deep burial of Asian continental crust beneath the Pamir imaged with local earthquake tomography. *Earth and Planetary Science Letters*, *384*, 165–177. <https://doi.org/10.1016/j.epsl.2013.10.013>
- Sippl, C., Schurr, B., Yuan, X., Mechie, J., Schneider, F. M., Gadoev, M., et al. (2013). Geometry of the Pamir-Hindu Kush intermediate-depth earthquake zone from local seismic data. *Journal of Geophysical Research: Solid Earth*, *118*(4), 1438–1457. <https://doi.org/10.1002/jgrb.50128>
- Smit, J. H. W., Brun, J. P., & Sokoutis, D. (2003). Deformation of brittle-ductile thrust wedges in experiments and nature. *Journal of Geophysical Research*, *108*(B10), 2480. <https://doi.org/10.1029/2002JB002190>
- Stübner, K., Ratschbacher, L., Rutte, D., Stanek, K., Minaev, V., Wiesinger, R., et al. (2013). The giant Shakh dara migmatitic gneiss dome, Pamir, India-Asia collision zone. 1: Geometry and kinematics. *Tectonics*, *32*, 948–979. <https://doi.org/10.1002/tect.20057>
- Talbot, C. J. (1998). Extrusions of Hormuz salt in Iran. In D. J. Blundell & A. C. Scott (Eds.), *Lyell: The past is the key to the present*. (Vol. 143, pp. 315–334). London, UK: Geological Society, London, Special Publications <https://doi.org/10.1144/GSL.SP.1998.143.01.21>, 1
- Thomas, J.-C., Chauvin, A., Gapais, D., Bazhenov, M. L., Perroud, H., Cobbold, P. R., & Burtman, V. S. (1994). Paleomagnetic evidence for Cenozoic block rotations in the Tadjik depression (Central Asia). *Journal of Geophysical Research*, *99*(B8), 15,141–15,160.
- Thomas, J. C., Cobbold, R. R., Wright, A., & Gapais, D. (1996). Cenozoic tectonics of the Tadjik depression, Central Asia. In A. Yin, & T. M. Harrison (Eds.), *The tectonic evolution of Asia*, (pp. 191–210). Cambridge, UK: Cambridge University Press.
- Thomas, J. C., Gapais, D., Cobbold, P. R., Meyer, V., & Burtman, V. S. (1994). Tertiary kinematics of the Tadjik depression (central Asia): Inferences from fault and fold patterns. In F. Roure, N. Ellouz, V. S. Shein, & I. Skvortsov (Eds.), *Geodynamic evolution of sedimentary basins*, International Symposium, (pp. 171–180). Moscow: Institut Francais du Petrole, Rueil-Malmaison, France.
- Vlasov, N. G., Dyakov, Y. A., & Cherev, E. S. (1991). *Geological map of the Tajik SSR and adjacent territories, 1:500,000, Vsesojuznoi Geol.* Saint Petersburg: Inst. Leningrad.
- Woodward, N. B., Boyer, S. E., & Suppe, J. (1989). Balanced cross-sections: An essential technique in geological research and exploration. In *Short Course in Geology, AGU Short Course Series*, (Vol. 6, pp. 1–132). Washington, DC: American Geophysical Union.
- Zubovich, A. V., Wang, X.-Q., Scherba, Y. G., Schelochkov, G. G., Reilinger, R., Reigber, C., et al. (2010). GPS velocity field of the Tien Shan and surrounding regions. *Tectonics*, *29*(6), TC6014. <https://doi.org/10.1029/2010TC002772>